Received: 2 April 2021 | Revised: 30 July 2021 | Accepted: 9 August 2021

DOI: 10.1002/ar.24777

SPECIAL ISSUE ARTICLE

The Anatomical Record

WILEY

Reevaluation of the cranial osteology and phylogenetic position of the early crocodyliform *Eopneumatosuchus colberti*, with an emphasis on its endocranial anatomy

Keegan M. Melstrom[1] | **Alan H. Turner**[2] | **Randall B. Irmis**[3,4]

[1]Dinosaur Institute, Natural History Museum of Los Angeles County, Los Angeles, California, USA

[2]Department of Anatomical Sciences, Stony Brook University, Stony Brook, New York, USA

[3]Natural History Museum of Utah, University of Utah, Salt Lake City, Utah, USA

[4]Department of Geology and Geophysics, University of Utah, Salt Lake City, Utah, USA

Correspondence
Keegan M. Melstrom, Dinosaur Institute, Natural History Museum of Los Angeles County, 900 West Exposition Boulevard, Los Angeles, CA 90007.
Email: keeganmelstrom@gmail.com

Funding information
Division of Environmental Biology, Grant/Award Numbers: 1754596, 1754659; National Science Foundation, Grant/Award Number: Graduate Research Fellowship; University of Utah

Abstract

Eopneumatosuchus colberti Crompton and Smith, 1980, known from a single partial skull, is an enigmatic crocodylomorph from the Lower Jurassic Kayenta Formation. In spite of its unique morphology, an exceptionally pneumatic braincase, and presence during a critical time period of crocodylomorph evolution, relatively little is known about this taxon. Here, we redescribe the external cranial morphology of *E. colberti*, present novel information on its endocranial anatomy, evaluate its phylogenetic position among early crocodylomorphs, and seek to better characterize its ecology. Our examination clarifies key aspects of cranial suture paths and braincase anatomy. Comparisons with related taxa (e.g., *Protosuchus haughtoni*) demonstrate that extreme pneumaticity of the braincase may be more widespread in protosuchids than previously appreciated. Computed tomography scans reveal an endocranial morphology that resembles that of other early crocodylomorphs, in particular the non-crocodyliform crocodylomorph *Almadasuchus figarii*. There are, however, key differences in olfactory bulb and cerebral hemisphere morphology, which demonstrate the endocranium of crocodylomorphs is not as conserved as previously hypothesized. Our phylogenetic analysis recovers *E. colberti* as a close relative of *Protosuchus richardsoni* and *Edentosuchus tienshanensis*, contrasting with previous hypotheses of a sister group relationship with Thalattosuchia. Previous work suggested the inner ear has some similarities to semi-aquatic crocodyliforms, but the phylogenetic placement of *E. colberti* among protosuchids with a terrestrial postcranial skeletal morphology complicates paleoecological interpretation.

KEYWORDS

Crocodyliformes, Crocodylomorpha, Early Jurassic, endocast, Kayenta Formation, pneumaticity

1 | INTRODUCTION

The early evolution of Crocodyliformes represents a crucial moment in the crocodylomorph radiation, when cursorial, generally small-bodied faunivores with upright posture diversified into a wide variety of ecological roles including those with anatomical specializations associated with the clade through the Mesozoic and Cenozoic (e.g., Bronzati

et al., 2015; Melstrom & Irmis, 2019; Schwab et al., 2020; Toljagic & Butler, 2013; Wilberg et al., 2019). Though crocodyliforms originated by the middle Norian during the Late Triassic Epoch (e.g., Irmis et al., 2013; Martínez et al., 2019), their diversification and initial evolutionary specializations largely occurred during the Early Jurassic Epoch, in the wake of the end-Triassic mass extinction. During that time, the first semiaquatic and aquatic crocodyliform taxa appeared in the fossil record (Bronzati et al., 2015; Irmis et al., 2013; Schwab et al., 2020; Tykoski et al., 2002), and there was a divergence in diet, with the appearance of both marine macropredators and terrestrial herbivores (Melstrom & Irmis, 2019; Wilberg et al., 2019).

A key fossil archive documenting this evolutionary phase of early crocodyliforms is the uppermost Triassic-Lower Jurassic Glen Canyon Group, exposed on the Colorado Plateau of the southwestern United States (e.g., Sues et al., 1994; Tykoski, 2005). In particular, the Lower Jurassic Kayenta Formation preserves a remarkable assemblage of crocodylomorphs and other nonmarine tetrapods, including lissamphibians, tritylodont mammaliamorphs, early mammaliaforms, lepidosauromorphs, turtles, pterosaurs, and saurischian and ornithischian dinosaurs (Breeden III & Rowe, 2020; Curtis & Padian, 1999; Hoffman & Rowe, 2018; Jenkins et al., 1983; Marsh et al., 2014; Marsh & Rowe, 2018, 2020; Padian, 1984; Sterli & Joyce, 2007; Sues, 1986; Sues et al., 1994). The vast majority of these specimens are from the "silty facies" exposed in northern Arizona within the Navajo Nation. At least five crocodylomorph taxa are present in the Kayenta Formation, comprising a diversity of clades, including non-crocodyliform crocodylomorphs ("sphenosuchians"), protosuchids, and a potential goniopholidid (Clark & Sues, 2002; Crompton & Smith, 1980; Sues et al., 1994; Tykoski, 2005; Tykoski et al., 2002; Wilberg et al., 2019).

Perhaps the most enigmatic taxon from this assemblage is *Eopneumatosuchus colberti* Crompton & Smith, 1980. Discovered in 1979, this taxon is known from only a single specimen (MNA V2460) comprising a partial braincase and skull roof (Crompton & Smith, 1980). Although fragmentary, *E. colberti* is noteworthy for its eponymous well-pneumatized braincase and large supratemporal fenestrae. Subsequent studies have largely overlooked this taxon despite its unusual morphology and potential for documenting the early evolution of the crocodyliform braincase. Few phylogenetic analyses have included *E. colberti*; those that have recover it in two markedly different positions, either among a typically paraphyletic grade of "protosuchians" near the base of Crocodyliformes (Bronzati et al., 2012; Clark, 1994; Fiorelli & Calvo, 2008; Wu et al., 2001), or as the sister taxon of Thalattosuchia, a large clade of marine crocodylomorphs (Foffa et al., 2019; Johnson et al., 2020; Ősi et al., 2018; Sachs et al., 2019; Schwab et al., 2020). Thus, *E. colberti* could be critical for clarifying the timing of the diversification of certain crocodyliform lineages and documenting key cranial character state acquisitions in these groups.

The well-preserved braincase of *E. colberti* is particularly intriguing because there has been a marked increase in studies exploring the evolution of soft tissue structures within the endocranium of crocodylomorphs and their close relatives (e.g., Bona et al., 2017; Bronzati et al., 2021; Erb & Turner, 2021; Holliday et al., 2020; Holloway et al., 2013; Kley et al., 2010; Lautenschlager & Butler, 2016; Lessner & Stocker, 2017; Nesbitt et al., 2017; Pierce et al., 2017). Those studies documented key patterns in crocodylomorph endocranial anatomy, such as broad changes in endocast morphology, modifications of semicircular canal shape related to habitat, and the expansion of cranial pneumatization (Bronzati et al., 2021; Brusatte et al., 2016; Erb & Turner, 2021; Fonseca et al., 2020; Herrera et al., 2018; Kley et al., 2010; Lautenschlager & Butler, 2016; Leardi et al., 2020; Pierce et al., 2017; Porter et al., 2016; Schwab et al., 2020; Serrano-Martínez et al., 2019, 2019b, 2020; Sertich & O'Connor, 2014; Watanabe et al., 2019). Given its hypothesized placement near the base of Crocodyliformes, *E. colberti* has the potential to elucidate one or more of these evolutionary transitions. This is only possible with a better understanding of the cranial morphology and phylogenetic position of the taxon.

Here, we reexamine the cranial osteology of *E. colberti* and describe previously unobserved aspects of internal anatomy, including pneumaticity and neuroanatomy, and compare these observations to other early crocodylomorph taxa. We then utilize these new data to conduct a phylogenetic analysis to help resolve the phylogenetic position of this critical taxon, rediagnose the taxon in a modern comparative framework, and discuss its implications for the early evolution of crocodyliforms.

2 | MATERIALS AND METHODS

2.1 | Computed tomography

The holotype and only known skull of *Eopneumatosuchus colberti* was μCT scanned at the University of Utah Preclinical Imaging Core Facility on March 1, 2012. It was scanned using a Siemens INVEON μCT scanner at a voxel resolution of 97 μm, a voltage of 80 kVp, and a current of 500 μA, comprising a total of 1,128 slices. We segmented the skull, endocranial cavity, and nerve paths in Avizo Lite (Windows Version 2020.1). 3D models and original μCT scans are available for download on MorphoSource (www.morphosource.org; https://doi.org/10.17602/M2/M365516).

2.2 | Phylogenetic analysis

To test the phylogenetic placement of *E. colberti*, we have integrated the taxon into the recent early crocodylomorph-focused dataset of Wilberg et al. (2019), a modified version of the dataset of Wilberg (2015) (Appendix S1, Supporting Information). No other modifications to the dataset were made. We used 97 crocodylomorph taxa and 407 characters (41 ordered) in the analysis, with *Gracilisuchus stipanicicorum* and *Postosuchus kirkpatricki* used to root the most parsimonious trees. The dataset was treated with equally weighted parsimony analysis implemented in TNT v. 1.5 (Goloboff et al., 2003; Goloboff & Catalano, 2016) (see discussion by Goloboff et al., 2019). A heuristic tree search strategy was conducted using multiple replications of new technology searches until it produced 20 hits to the shortest length (xmult = hits 20). The best trees obtained at the end of the xmult search were subjected to a final round of TBR branch swapping. Zero length branches were collapsed if they lacked support under any of the most parsimonious reconstructions (i.e., rule 1 of Coddington & Scharff, 1994).

2.3 | Institutional abbreviations

AMNH FARB, American Museum of Natural History, Fossil Amphibians, Reptiles, and Birds, New York, NY, United States; BP, Bernard Price Institute for Palaeontological Research, Johannesburg, South Africa; GMPKU, Geological Museum, School of Earth and Space Sciences, Peking University, Beijing, People's Republic of China; IDEAN, Instituto de Estudios Andinos "Don Pablo Groeber," Universidad de Buenos Aires, Buenos Aires, Argentina; IVPP, Institute of Vertebrate Paleontology and Paleoanthropology, Beijing, People's Republic of China; LACM, Natural History Museum of Los Angeles County, Los Angeles, CA, United States; MCZ, Museum of Comparative Zoology, Harvard University, Cambridge, MA, United States; MNA, Museum of Northern Arizona, Flagstaff, AZ, United States; NHMUK PV, Natural History Museum, London, United Kingdom; SAM, Iziko South African Museum, Cape Town, South Africa; SMNS, Staatliches Museum für Naturkunde Stuttgart, Stuttgart, Germany.

3 | SYSTEMATIC PALEONTOLOGY

Archosauria Cope, 1869 sensu Gauthier, 1986
Pseudosuchia Zittel, 1887 sensu Gauthier & Padian, 1985
Crocodylomorpha Hay, 1930 sensu Nesbitt, 2011
Crocodyliformes Hay, 1930 sensu Benton & Clark, 1988 and Sereno et al., 2001
Protosuchidae Brown, 1934 sensu Benton & Clark, 1988
Eopneumatosuchus colberti Crompton & Smith, 1980

3.1 | Holotype

MNA V2460, posterior portion of a skull, consisting of the skull roof medial and posterior to the orbits, and partial braincase missing the quadrate-quadratojugal complex.

3.2 | Revised diagnosis

Eopneumatosuchus colberti can be distinguished from other early crocodylomorphs by the following unique combination of character states: differs from all other crocodylomorphs except *Enaliosuchus macrospondylus* and geosaurines in that the distance between the posterior processes of the nasals is nearly as long as the distance from the posterior process of the nasal to the anterior margin of the supratemporal fossa (character 35, state 1); differs from all other early crocodylomorphs with the exception of *Sphenosuchus acutus* and thalattosuchians in possessing a supratemporal fenestra that is larger than the orbit, but less than twice as long as wide (character 55, state 1) as well as a supratemporal fossa that reaches as far anteriorly as the postorbital (character 58, state 2); differs from all other early crocodylomorphs except *Hsisosuchus chungkingensis*, *H. dashanpuensis, Sichuanosuchus shuhanensis*, and *Shantungosuchus hangjinensis* in displaying a thin posterior edge of the supratemporal fenestra (character 62, state 1); differs from all other crocodylomorphs except thalattosuchians, tethysuchians, and *Gavialis* in having a maximum frontal interorbital width greater than 50% of skull width at the orbit (character 110, state 1); differs from other early crocodylomorphs except *Hsisosuchus chungkingensis* by possessing an anterior process of the frontal that extends far anterior to the anterior margin of the orbit (character 113, state 0); differs from all other crocodylomorphs except dyrosaurids in displaying an extremely long basisphenoid rostrum (character 248, state 1); and differs from all other crocodyliforms and thalattosuchians in possessing lateral eustachian tubes that are not enclosed between the basisphenoid and basioccipital (character 246, state 0) as well as a basisphenoid-exoccipital suture that is absent (character 259, state 0).

3.3 | Potential additional material

No additional material has been formally referred to this taxon. Sues et al. (1994, p. 288) mentioned but did not describe, diagnose, or figure "several isolated bones from

the type locality and a partial skeleton (MCZ 8895) from another site" that might be referable to the species. The "several isolated bones" Sues et al. (1994) mentioned were collected by Jim Clark and include an ilium, several large osteoderms, and an isolated astragalus (Clark, 1986). MCZ 8895 was collected by Charles Scharff from the Gold Springs area (Clark, 1986). We have not examined this material and because there is no direct overlap with the holotype specimen it cannot be referred to *E. colberti*.

3.4 | Locality, horizon, and age

Eopneumatosuchus colberti (MNA V2460) was discovered at MNA locality 744-1 (Seller Spring), approximately 5 miles north of Dinosaur Canyon and 11 miles northeast of the town of Cameron, Coconino County, AZ, United States, within the Navajo Nation (Figure 1). The site is located in the "silty facies" of the Lower Jurassic Kayenta Formation, but there is some confusion in the literature about its exact stratigraphic position. Crompton and Smith (1980, p. 197) stated the specimen was found "in the silty facies at the base of the Kayenta Formation"; in contrast, Clark and Fastovsky (1986, p. 291) said the site "lies in blue silts at the base of the upper portion of the silty facies, approximately 3 m above the top of Kayenta beds with sandstones of Dinosaur Canyon lithology."

Locality data on file at MNA indicate that locality 744-1 is situated among a set of low "silty facies" badlands southwest of Seller Spring itself, and just west of the main Ward Terrace escarpment. Depending on the exact location at which the skull was discovered, this indicates that *E. colberti* was discovered between 15 and 35 m above the base of the Kayenta Formation. This places it slightly higher in section than the holotype specimen of the theropod dinosaur *Dilophosaurus wetherilli*, but lower in section than most of the classic vertebrate fossil sites further south near Gold Spring and Rock Head (Clark & Fastovsky, 1986; Marsh, 2018; Marsh & Rowe, 2018, 2020).

There is widespread consensus that the Kayenta Formation is Early Jurassic in age, but more specific constraints are limited. In this part of northeastern Arizona, the formation is unconformably underlain by the Moenave Formation; chemical abrasion-thermal ionization mass spectrometry (CA-TIMS) U–Pb detrital zircon ages, chemostratigraphy, and magnetostratigraphy indicate that the top of the Moenave Formation is late Hettangian or earliest Sinemurian in age (Donohoo-Hurley et al., 2010; Molina-Garza et al., 2003; Suarez et al., 2017). Magnetostratigraphic data from the Springdale Sandstone (base of the Kayenta Formation) (Molina-Garza et al., 2003; Steiner, 2014) could correlate to multiple parts of the Sinemurian–Pliensbachian magnetic polarity timescale (cf. Moreau et al., 2002; Yang et al., 1996), and paleomagnetic data from the silty facies of the Kayenta Formation near the type locality of *E. colberti* (see Bazard & Butler, 1991) were not placed in stratigraphic context, so cannot be used for magnetostratigraphic correlation. New laser ablation-inductively coupled plasma mass spectrometry (LA-ICPMS) U–Pb detrital zircon ages from the Kayenta Formation of northern Arizona indicate the top of the unit could be as late as Toarcian in age, but are consistent with a Sinemurian–Pliensbachian age for the lower part of the formation, including the *E. colberti* type locality (Marsh, 2015, 2018; Marsh et al., 2014). That said, these data should be interpreted cautiously, because the geologic uncertainty of LA-ICPMS U–Pb zircon ages is an order of magnitude larger than their analytical uncertainty (e.g., Herriott et al., 2019; Rasmussen et al., 2020; von Quadt et al., 2014). In summary, the balance of evidence suggests a Sinemurian–Pliensbachian age for the type locality of *E. colberti*, which would place it between ~199.5 and ~184 Ma based on our current understanding of the geologic timescale (i.e., Hesselbo et al., 2020).

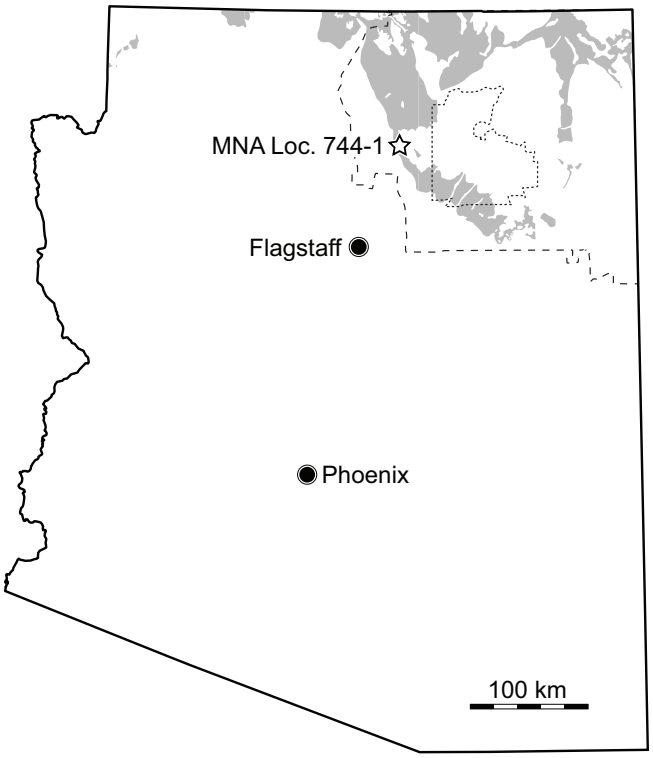

FIGURE 1 Map of the state of Arizona (United States), Hopi Reservation (fine dotted line), and Navajo Nation (dotted line) showing the holotype locality of *Eopneumatosuchus colberti*. Gray shading indicates the distribution of outcrops of the Glen Canyon Group, including the Lower Jurassic Kayenta Formation. Modified from Richard et al. (2000)

4 | DESCRIPTION

4.1 | External cranial osteology

The specimen MNA V2460 of *Eopneumatosuchus colberti* comprises the central portion of the skull table and a partial braincase (Figures 2–6). The anterior portion of this specimen, described in detail in the initial publication, consists of paired nasals, which are elongate and narrow (Crompton & Smith, 1980). These elements are marked by grooves and pits, which characterize the skulls of most crocodyliforms but are absent in early crocodylomorphs, such as *Dibothrosuchus elaphros*, *Sphenosuchus acutus*, and *Junggarsuchus sloani* (Walker, 1990, figs. 2–6; Wu & Chatterjee, 1993, figs. 2 and 4; Clark et al., 2004, fig. 2). The contact with the premaxillae and maxillae is not preserved. The anterior portion of the nasals remains partially covered by a hematite layer, which obscures much of their morphology (Figure 2). Posteriorly, the nasals contact both the frontal and prefrontal along a suture that is "W"-shaped in dorsal view, being slightly separated by an anterior projection of the frontals, similar to the condition observed in *D. elaphros* (IVPP V 7907; Wu & Chatterjee, 1993). The divided nasals and frontals

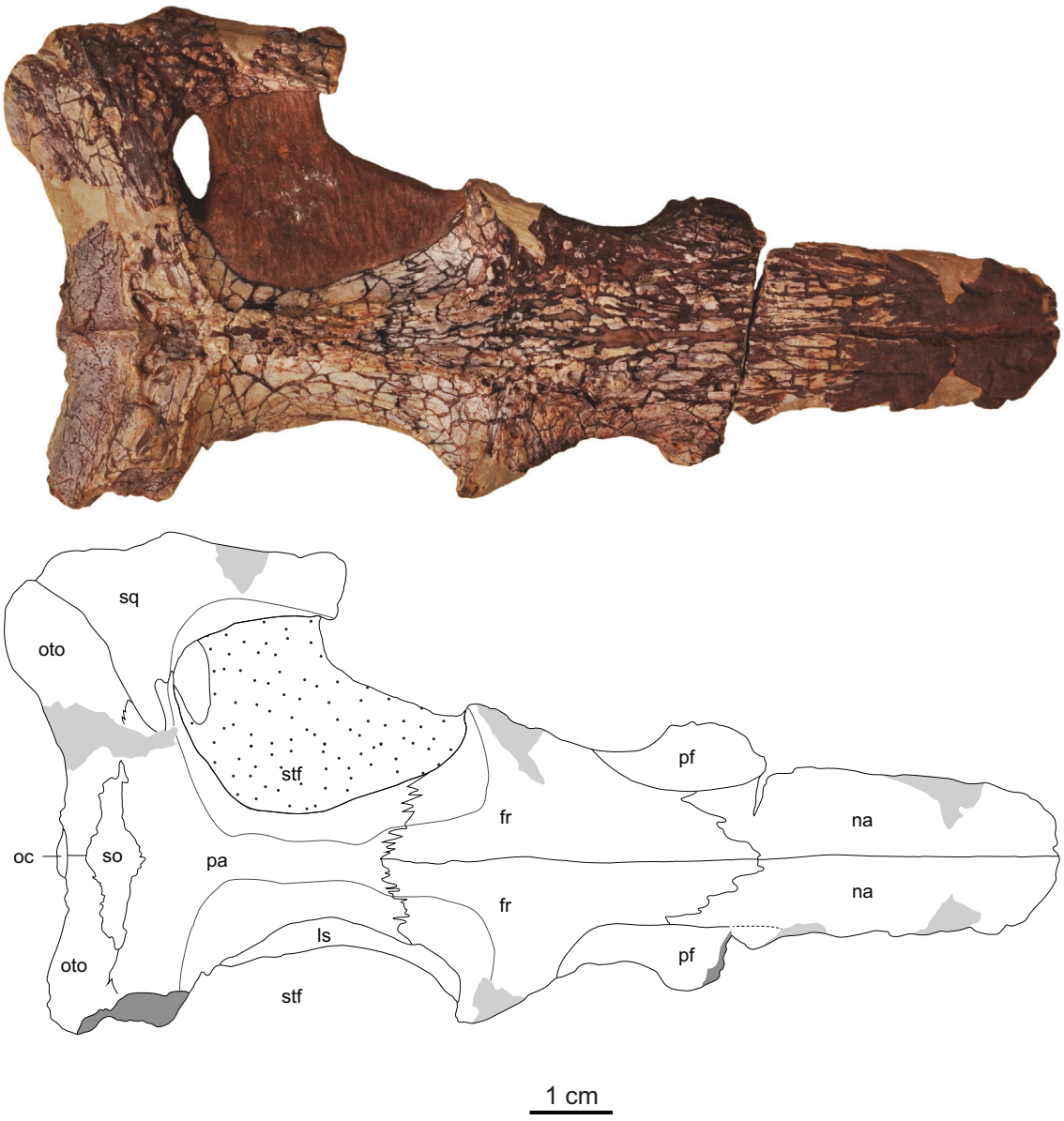

FIGURE 2 Skull of the holotype of *Eopneumatosuchus colberti* (MNA V2460) in dorsal view. In the accompanying line drawing, stippling indicates matrix, light gray denotes reconstructed areas, and dark gray indicates broken surfaces. fr, frontal; ls, laterosphenoid; na, nasal; oc, occipital condyle; oto, otoccipital; pa, parietal; pf, prefrontal; pr, prootic; scp, subcapsular process; so, supraoccipital; sq, squamosal; stf, supratemporal fenestra

are not bowed dorsoventrally, thus creating a nearly horizontal skull table and dorsal surface of the snout.

Skull roof elements preserved in MNA V2460 include prefrontals, frontals, the parietal, and the left squamosal (Figure 2). Neither of the postorbitals are preserved, contrary to the descriptive text of Crompton and Smith (1980). The prefrontals are relatively long, mediolaterally narrow, and taper slightly posteriorly. These elements contact the nasals and frontals along their long medial border, whereas their lateral border forms over half of the dorsal orbital rim, as is the case in some early crocodylomorphs and protosuchians (e.g., *Orthosuchus stormbergi*) (Nash, 1968, fig. 1; Wu & Chatterjee, 1993, fig. 2). There is no preserved indication of a palpebral facet. In lateral view (Figure 6a), the beginnings of a prefrontal pillar are evident and circumscribe the anterior boundary of the orbit.

The frontals are paired as in all nonmesoeucrocodylians (Clark, 1994). They are separated by a relatively wide median suture (Figure 2), which is also observed in other early crocodylomorphs, such as *Almadasuchus figarii*, *D. elaphros*, and *Hesperosuchus agilis* (Pol et al., 2013, fig. 1; Sues et al., 2003, fig. 2; Wu & Chatterjee, 1993, fig. 2). The frontals are anteroposteriorly longer than mediolaterally wide and sculptured, similar to the condition of many other crocodylomorphs. The dorsal surface ornamentation consists of partially interconnected circular pits. There is no midline ridge, unlike the prominent structures in *D. elaphros* and *S. acutus* (Walker, 1990, fig. 6; Wu & Chatterjee, 1993, figs. 2, 4) or low ridges of *Gobiosuchus kielanae* and *Zaraasuchus shepardi* (Osmólska et al., 1997, figs. 2, 6; Pol et al., 2004, fig. 1), nor is there a midline depression (Figure 2). The frontals form the posteromedial half of the orbital margins and the preserved anterior margin of the supratemporal fenestrae. The medial margin of the orbits are approximately half the length of those of the supratemporal fenestrae. Some non-crocodyliform crocodylomorphs, such as *S. acutus*, and thalattosuchians also exhibit relatively large supratemporal fenestrae, which contrasts with some crocodyliforms from the Early Jurassic (e.g., *Protosuchus richardsoni*, Figure 3b) and younger basal crocodyliforms, such as *Z. shepardi* (Pol & Norell, 2004, figs. 2, 3). Similarly, *E. colberti* appears to lack the greatly enlarged orbits observed in Late Triassic, Early Jurassic, and Late Jurassic taxa such as *Dromicosuchus grallator* (UNC 15574), *P. richardsoni* (AMNH FARB 3024), *P. haughtoni* (BP/1/4770), and *Fruitachampsa callisoni* (LACM 120455; Figure 3; Clark, 2011). The postorbital processes of the frontals flare slightly beyond the preserved lateral extent of the prefrontals. Immediately adjacent to the supratemporal fossa there is a narrow groove present on the postorbital process of the frontal, which we interpret to be related to the articulation of the postorbital element. The frontal extends approximately one third of the way along the supratemporal fenestra (Figure 2). The frontoparietal suture is heavily interdigitated but nearly straight across the interfenestral bar. Immediately lateral and anterior to the frontoparietal suture the dorsal edge of the laterosphenoid is exposed. There is no indication that the postorbital would have reached far into the supratemporal fenestra or have reached the parietal.

As previously noted, the supratemporal fenestrae in *E. colberti* are relatively large compared to other basal crocodyliforms (e.g., *P. haughtoni*, *P. richardsoni*, *F. callisoni*, and *Z. shepardi*), with the long axis of the left fenestra measuring approximately 3.5 cm (Figure 3). Each fenestra is surrounded by a shallow supratemporal fossa. The fossa reaches anteriorly to the level of the postorbital process of the frontal such that the posterolateral corner of the frontal is impressed by the fossa (Holliday et al., 2020). Based on the preserved elements, the supratemporal fenestra is subrectangular in shape with the medial and lateral margins roughly parallel with one another. The supratemporal fossa terminates posteriorly well before the posteriormost edge of the parietal, as in basal crocodyliforms such as *P. richardsoni*, *O. stormbergi*, and *Si. shuhanensis* and in contrast to the condition in early diverging crocodylomorphs like *He. agilis* and *A. figarii*, in which the fossa extends right to the posterior parietal border and essentially contacts the supraoccipital bone (Figure 3; Colbert & Mook, 1951, fig. 5; Leardi et al., 2020, fig. 1; Nash, 1968, fig. 1; Wu et al., 1997, fig. 1). Thus, there is a narrow supratemporal fossa present on the medial margin of the supratemporal fenestra that terminates near the parietal-squamosal suture. Absent in *E. colberti* is a distinct posterior ridge marking the boundary of the supratemporal fenestra like that present in "sphenosuchian" taxa (e.g., *He. agilis*, *J. sloani*, *T. gracilis*) as well as other early crocodylomorphs like *A. figarii* (Crush, 1984, fig. 1; Clark et al., 2004, fig. 2; Pol et al., 2013, fig. 1).

The parietal is unpaired as in all crocodylomorphs (Clark, 1994) and forms the posterior two-thirds of the supratemporal fenestra (Figure 2). Anterolaterally, the contact between the parietal, frontal, and laterosphenoid is exposed within the supratemporal fenestra. The frontoparietal suture is a simple interdigiting suture, widely exposed within the supratemporal fossa, with the laterosphenoid underlying the two elements (Figures 2 and 4). There is no long anterior process wedging between the frontal and laterosphenoid like that observed in *Pholidosaurus purbeckensis*, *Pelagosaurus typus*, and many other thalattosuchians (Jouve, 2009). The dorsal exposure of the parietal portion of the interfenestral bar is well developed. It is flat and ornamented in the same manner as the frontal and the noninterfenestral portion of the parietal. The parietal does not form a ridge-like

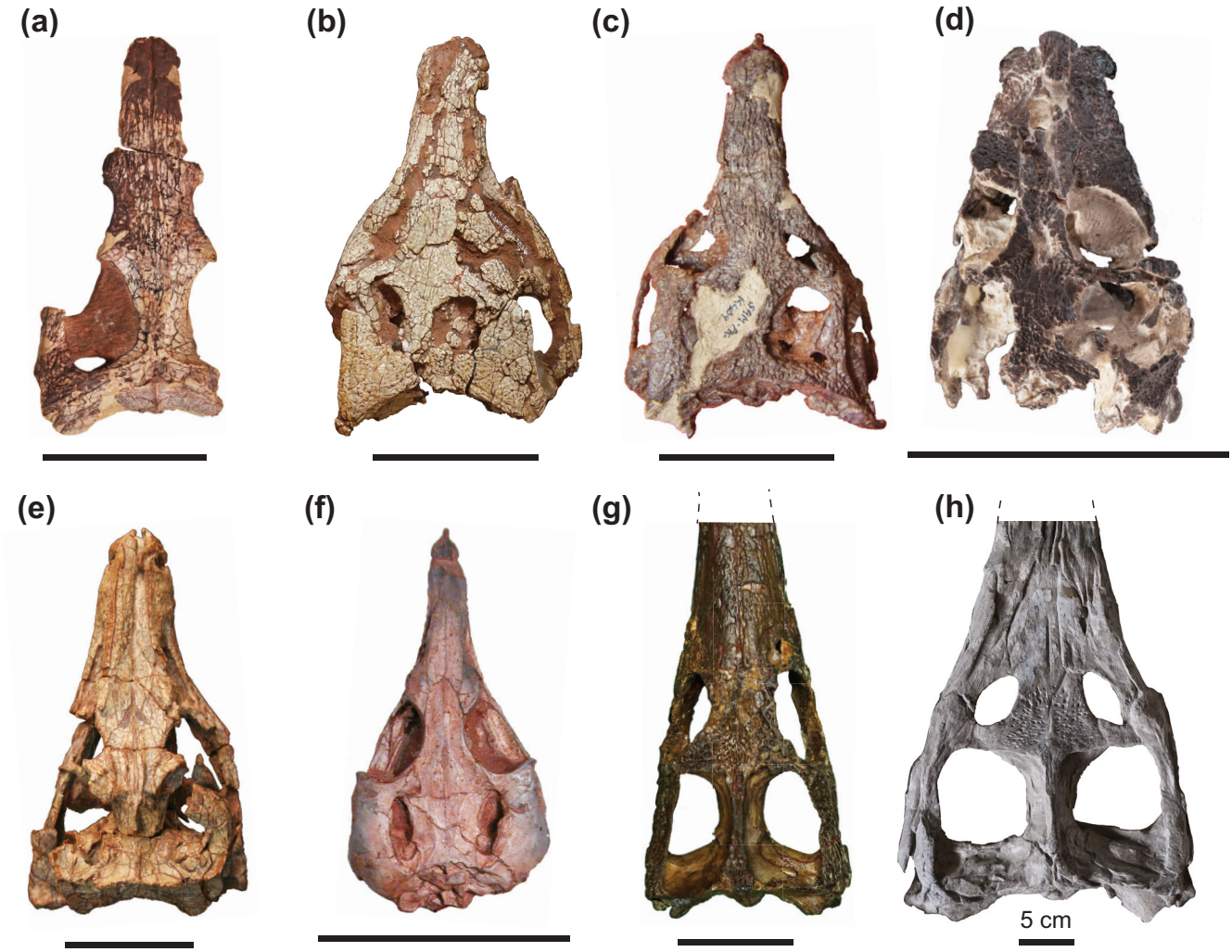

FIGURE 3 Comparison of the skulls of early crocodylomorphs in dorsal view. (a) *Eopneumatosuchus colberti* (MNA V2460). (b) *Protosuchus richardsoni* (AMNH FARB 3024). (c) *Orthosuchus stormbergi* (SAM-PK-K409). (d) *Fruitachampsa callisoni* (LACM 120455). (e) *Dibothrosuchus elaphros* (IVPP V 7907). (f) *Litargosuchus leptorhynchus* (BP-1-5237). (g) *Pelagosaurus typus* (NHMUK PV OR 32599). (h) *Macrospondylus bollensis* (SMNS 54063). Dotted lines represent continuation of snouts (g and h removed to facilitate comparison with a–d). Photo of *Fruitachampsa callisoni* and *Orthosuchus stormbergi* courtesy of S. Abramowicz (LACM) and J. M. Leardi (IDEAN), respectively

sagittal crest like that in "sphenosuchian" taxa (e.g., *He. agilis*, *D. elaphros*, *J. sloani*) or *A. figarii* (Wu & Chatterjee, 1993, fig. 2; Clark et al., 2004, fig. 2; Pol et al., 2013, fig. 1). The interfenestral bar is widest anteriorly where it is formed from the frontal; posteriorly it narrows slightly to be approximately 0.5 cm wide. This morphology contrasts with the very broad interfenestral parietal seen in *P. richardsoni* and the early goniopholidid *Calsoyasuchus valliceps*, and most closely resembles the condition in *Pe. typus* (Figure 3g). The tapering is not as pronounced as that observed in more phylogenetically nested thalattosuchians such as *Macrospondylus* (i.e., "*Steneosaurus*") *bollensis* and *Platysuchus multiscrobiculatus* (Johnson et al., 2020). Within the supratemporal fossa, there is a small oval-shaped rugose contact facet on the parietal for the quadrate. Near this location on the left side of the specimen, there is an anteriorly visible opening likely representing the temporo-orbital foramen ("anterior temporal foramen" sensu; Walker, 1990, fig. 21). This opening is not visible in dorsal view. The parietal does not form a portion of this foramen, which is entirely bound by the prootic and squamosal. The posterior margin of the parietal is gently concave in dorsal profile with no supraoccipital exposure on the skull roof. The parietal is broad at the angle formed between the flat skull table and the occipital surface—it does not narrow posteriorly as in *G. kielanae* (Osmólska et al., 1997, fig. 3). The occipital exposure of the parietal is dorsoventrally narrow in contrast to the dorsoventral tall occipital exposure present in *A. figarii* (Pol et al., 2013, fig. 1). The parietal is more widely exposed on the occipital surface than the supraoccipital.

The left squamosal is preserved and is the lateral most element known in MNA V2460 (Figure 2). The squamosal can be divided into a flat dorsal surface and a posteriorly sloping occipital surface. Similar to other skull table elements, the dorsal surface of the squamosal is marked by distinct pitted ornamentation. The anterolateral process of the squamosal is elongate, significantly narrower than the width of supratemporal fenestra. The supratemporal fossa continues onto the anterior process of the squamosal for most of its preserved length and widens posteriorly. The dorsal surface forms a broad flat shelf overhanging a deep otic recess. In lateral view, there is an anteroposteriorly oriented groove along the anterior process of the squamosal, which we interpret to be for the external ear flap musculature. The ventral edge of this groove is more laterally placed than the dorsal edge of the groove as in many early crocodyliforms such as *P. richardsoni*, *O. stormbergi*, and *F. callisoni* (Clark, 2011; Colbert & Mook, 1951; Nash, 1968). Immediately posterior to the groove there is a small, laterally concave notch in the squamosal. The notch aligns with the inflection point of the dorsal surface and occipital surface of the squamosal. The squamosal has a short, poorly developed posterolateral process that is weakly deflected ventrally as in the crocodyliforms *P. richardsoni*, *Edentosuchus tienshanensis*, *F. callisoni*, and *Zosuchus davidsoni*. The occipital surface of the squamosal is not as dorsoventrally tall as in "sphenosuchians" like *D. elaphros* or *J. sloani*, nor as narrow as in taxa such as *P. typus* (Wu & Chatterjee, 1993, fig. 3; Clark et al., 2004, fig. 2; Pierce & Benton, 2006, fig. 3). On the occiput, the squamosal contacts the otoccipital in a nearly straight suture that dips ventrally towards the lateral margin of the skull (Figure 5). There is no evidence of a posttemporal fenestra, although a small portion of the posterior skull surface is missing in the region where one would expect it. The ventral surface of the squamosal bears three depressions (Figure 4). There is a shallow anterior depression situated between the groove for the external ear musculature and a long, interdigitated suture surface for the anterolateral process of the quadrate. Posterior to this, there is a second shallow depression that is associated with the posterolateral process. Situated medially to these two depressions is the third depression, which is deeper than the previous two and serves as the articulation surface for the posterodorsal process of the primary head of the quadrate. There is no indication that the squamosal would have contacted the quadrate posterior to the external acoustic meatus. This is typical of most early crocodyliforms (e.g., *P. richardsoni*, *O. stormbergi*, *F. callisoni*) and unlike the condition in *A. figarii* (Pol et al., 2013) and mesoeucrocodylians.

Neither quadrate is preserved in MNA V2460, but some aspects of its morphology can be deduced from the surrounding elements. Based on surfaces on the squamosal and lateral braincase wall, it is clear that the quadrate in *E. colberti* would have had a complex dorsal process typical of early crocodylomorphs. A shallow circular depression on the ventral aspect of the posterior part of the squamosal would have received the posterodorsal process of the quadrate (=ancestral quadrate head) (Figure 4). Extending anteriorly from this is a long, jagged sutural surface on the squamosal that indicates an equally long and well-developed anterodorsal process of the quadrate like that present in *D. elaphros* (Wu & Chatterjee, 1993, fig. 7) and crocodyliforms generally. The dorsomedial process (the medially directed portion of the primary head) has a fairly large lemniscate shaped contact facet with the prootic. The anterior margin of this facet is adjacent to the posterior edge of the laterosphenoid, thus indicating that the prootic would not have been visible on the lateral braincase wall, as in all crocodyliforms (Clark, 1994).

The neurocranium preserves a remarkable amount of detail. Many of the illustrations provided by Crompton and Smith (1980) are somewhat speculative, and a great deal more comparative data is available these 40 years since their original description. As such, we provide a number of corrections to past inaccurate reconstructions, although many of the initial details of the lateral braincase wall morphology still hold. Figure 5 shows our updated interpretation of the occipital surface of the skull compared to the original provided by Crompton and Smith (1980). The supraoccipital is mediolaterally wider than dorsoventrally tall and does not contact the foramen magnum, similar to the condition observed in *J. sloani* (Clark et al., 2004, fig. 2) and *P. haughtoni* (NHMUK R 8503; Whetstone & Whybrow, 1983). The supraoccipital also bears a median ridge visible in both dorsal and occipital view. The supraoccipital is not as wide as depicted by Crompton and Smith (1980) because the lateral edges extend only slightly beyond the lateral margins of the foramen magnum. The lateral edges are not tapered but instead are more vertically oriented at their contact with the squamosal. Crompton and Smith (1980) showed little occipital exposure of the squamosal with no squamosal/supraoccipital contact. The better preserved left side clearly shows a dorsoventrally tall occipital exposure of the squamosal along its substantial contact with the otoccipital. Both the left and right sides show the supraoccipital/squamosal contact.

The exoccipital and opisthotic are coossified into a single element—the otoccipital. The left and right otoccipitals meet at the midline to form the dorsal and lateral margins of the foramen magnum (Figure 5). The otoccipitals slope onto the base of the occipital condyle but do not form part of it. Although damaged near its midpoint, the left otoccipital preserves a complete

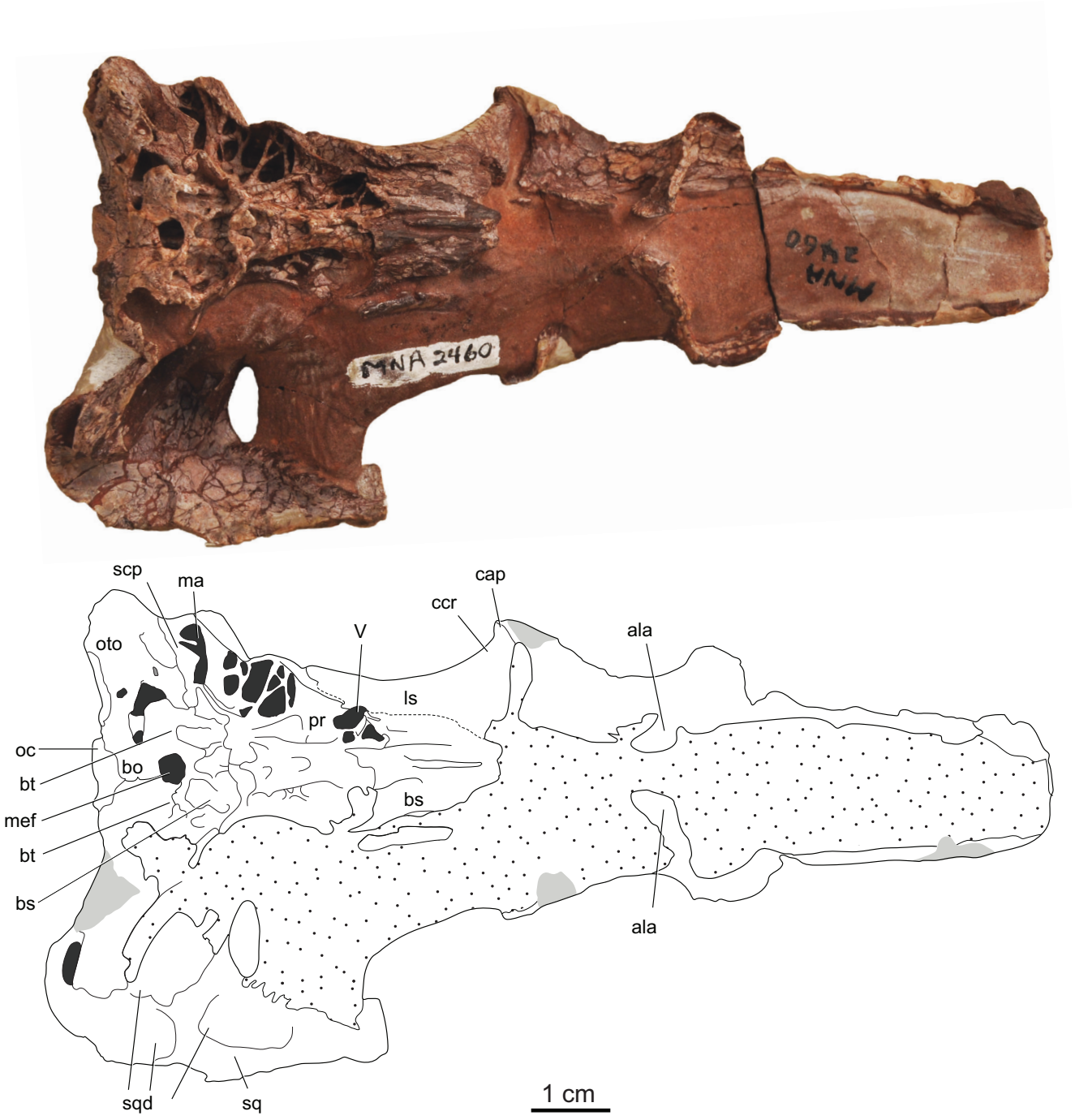

FIGURE 4 Skull of the holotype of *Eopneumatosuchus colberti* (MNA V2460) in ventral view. In the accompanying line drawing, stippling indicates matrix, light gray denotes reconstructed areas, and dark gray designates pneumatic openings. ala, articulation for the lacrimal; bo, basioccipital; bs, basisphenoid; bt, basal tubera; cap, capitate process; ccr, cotylar crest; ls, laterosphenoid; ma, mastoid antrum; mef, median eustachian foramen; oc, occipital condyle; oto, otoccipital; pr, prootic; scp, subcapsular process; sq, squamosal; sqd, squamosal depressions; V, trigeminal nerve

paroccipital process, which extends laterally farther than it does in *P. richardsoni* (UCMP 131827) but still not past the lateral margin of the skull table. There is no indication of a posttemporal fenestra at the junction of the paroccipital process, squamosal, and supraoccipital. Laterally, the paroccipital process slopes posteriorly, and beneath it lies a deep groove separating it from the remainder of the ventral margin of the otoccipital. Contrary to the interpretation of Crompton and Smith (1980), there would not have been the large dorsal portion of the otoccipital as depicted in their line reconstruction. Likewise, there is no indication on MNA V2460 that an

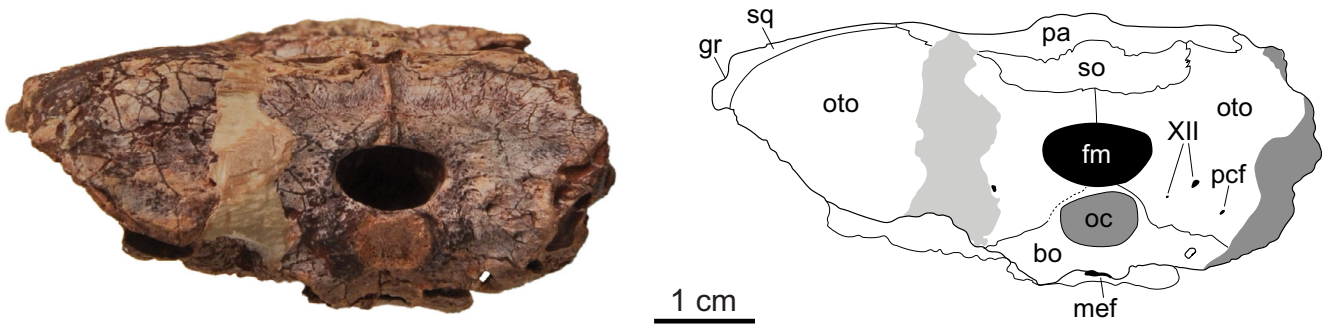

FIGURE 5 Skull of the holotype of *Eopneumatosuchus colberti* (MNA V2460) in posterior view. In the accompanying line drawing, light gray denotes reconstructed areas, gray indicates broken surfaces, and black indicates cranial opening. bo, basioccipital; fm, foramen magnum; gr, groove on the squamosal; mef, median eustachian foramen; oc, occipital condyle; oto, otoccipital; pa, parietal; pcf, posterior carotid foramen; so, supraoccipital; sq, squamosal; XII, hypoglossal nerve

extensive ventrolateral portion of the otoccipital would have been present either. Thus, it is our interpretation that *E. colberti* would have lacked the concave lateral edge of the ventrolateral flange of the otoccipital (like that seen in *P. richardsoni* [Clark, 1986]), and would not have had an otoccipital process articulating with the articular bone. Although the area around the ventral portion of the otoccipital is damaged, it is possible that the medial margin on the left side preserves a facet for contact with the quadrate.

Internally, there is a large subcapsular process extending dorsolaterally from the posterior aspect of the otic capsule back onto the paroccipital process and the ventrolateral part of the otoccipital. The subcapsular process and area ventral to it is extensively pneumatized in *E. colberti* (Figure 6). Anterior to the subcapsular process, the crista interfenestralis arises as a sharp ridge of bone near the origin of the paroccipital process. The crista is oriented at a 45° angle as it divides the area lateral to the vestibule (Figure 6). As in *S. acutus* and *P. haughtoni* (Busbey & Gow, 1984, fig. 8; Walker, 1990, fig. 24), this area is triangular in shape, and the smaller portion of this triangular space anterior to the crista interfenestralis is the fenestra ovalis. The larger portion posterior to the crista is the foramen pseudorotundum. The crista interfenestralis is an extension of the opisthotic, which expands into a ventrally directed boot at its contact with the basisphenoid and basioccipital. Posteromedial to this boot, the opisthotic sutures against the opisthotic-formed otic capsule in what Walker (1990) termed the loop-closure suture (as the opisthotic sutures "against itself" to form a loop of bone). The area deep to this space communicates with the metotic fissure. The posterior projection of the boot connects to the opisthotic-formed subcapsular process completing the ring of bone forming the foramen pseudorotundum. The area deep to this space communicates with the metotic fissure. There is a prominent groove that extends laterally as it runs along the dorsal surface of the subcapsular process (Figure 6). This groove that passes posteriorly divides the paroccipital process from the ventrolateral portion of the otoccipital (as described above). Given the origin of this groove near the metotic fissure, and its passage to the posterior aspect of the skull, we interpret this to be the path of cranial nerves IX, X, and XI. Thus, *E. colberti* lacks a defined foramen for these cranial nerves as in early crocodylomorphs (e.g., *S. acutus* and *D. elaphros*) and unlike *A. figarii* (Pol et al., 2013), crocodyliforms such as *P. richardsoni* (Clark, 1986), and thalattosuchians such as *P. typus*. Because there is no lateral contact between the paroccipital process and ventrolateral part of the otoccipital (or the quadrate for that matter), there is similarly no enclosed cranioquadrate canal for transmitting the communicating branch of the facial nerve (CN VII) and the lateral head vein. It is possible these structures traveled this space as well or just lateral to it. Our interpretations are similar to those proposed by Clark (1986) but quite unlike the reconstruction of Crompton and Smith (1980), which noted a distinctly enclosed cranioquadrate canal and a distinct foramen for the passage of cranial nerves IX and X on the posterior aspect of the occiput (Crompton & Smith, 1980, fig. 11.3).

A number of other foramina (or possible foramina) pierce the posterior aspect of the occiput in MNA V2460 (Figure 5). The foramen labeled as a "possible vascular vessel" in Crompton and Smith (1980, fig. 11.3) is here interpreted as the posterior carotid foramen. This foramen is in a position broadly similar to that in *A. figarii* (Pol et al., 2013, fig. 1), as well as in *P. richardsoni* and the Kayenta *Edentosuchus*-like taxon (Clark, 1986). Moreover, this foramen can be seen transmitting to an anteriorly opening foramen that is continuous with a groove running along the ventral aspect of the subcapsular process. This groove extends anteriorly to the level of the loop closure suture at which point it turns ventromedially

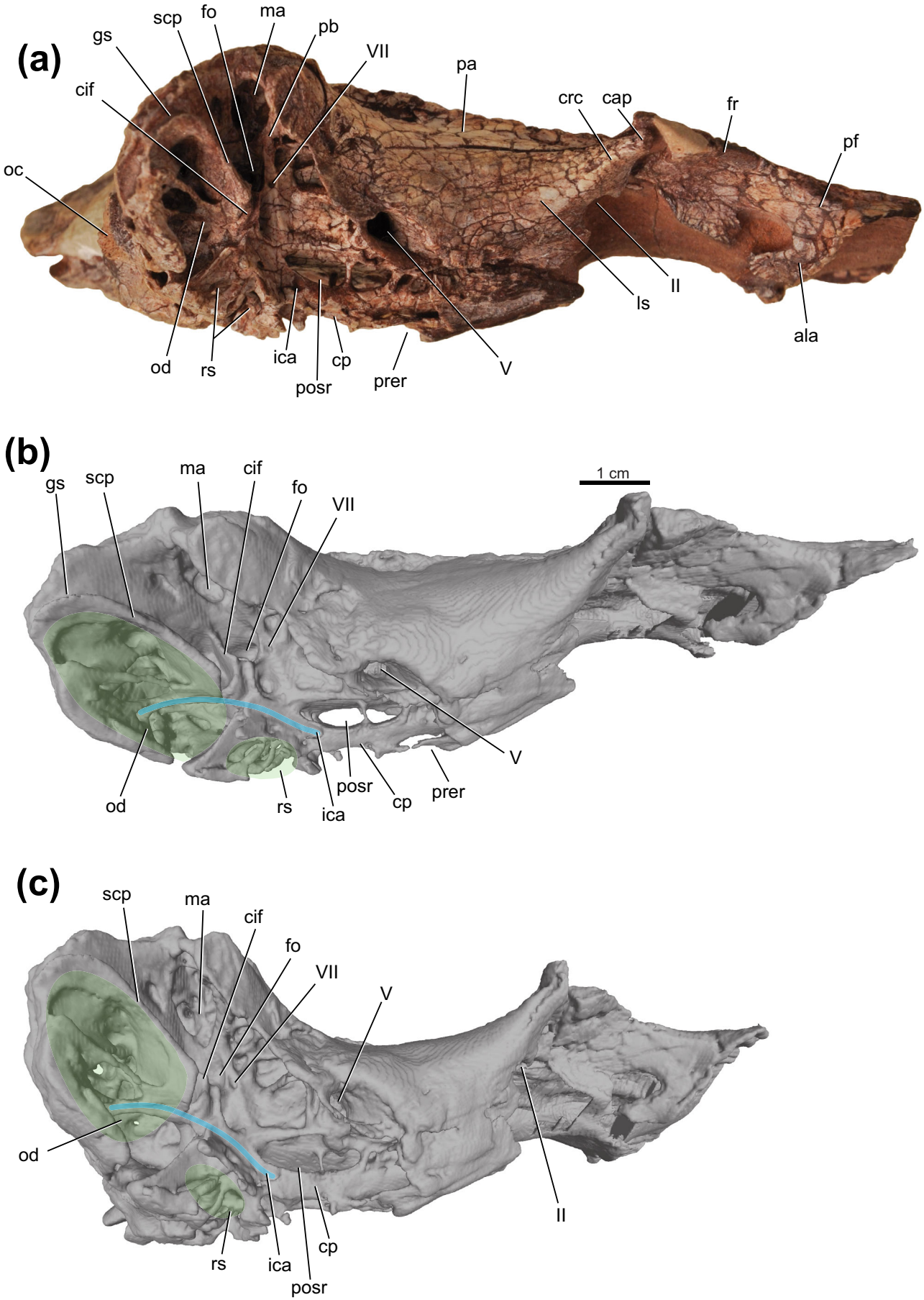

FIGURE 6 Legend on next page.

to transmit into an internal foramen in the basisphenoid posterior to the pituitary fossa, as would be expected for the course of the internal carotid artery.

Two small foramina are situated dorsomedially to the posterior carotid foramen. Only one of these was identified by Crompton and Smith (1980) as an exit for the hypoglossal nerve (CN XII), although we consider both of them to have served that purpose. The openings within the basioccipital labeled by Crompton and Smith (1980) for the cranial nerves IX + X, the internal carotid artery, and the lateral eustachian canal could not be replicated in our examination of MNA V2460 and instead appear to be the result of breakage of the specimen that exposed the pneumatic spaces ventral to the subcapsular process.

The basioccipital is triangle-shaped with a ventrolaterally directed sutural contact with the otoccipital. The occipital condyle is broken at its base (Figure 5). The basioccipital slopes anteroventrally at a 45° angle to terminate in a broad, weakly developed basal tubera as in *P. richardsoni* (Clark, 1986), and unlike the more vertically oriented basioccipital in *A. figarii* and "sphenosuchians" such as *D. elaphros* and *S. acutus* (Walker, 1990; Wu & Chatterjee, 1993, fig. 3; Pol et al., 2013, fig. 1). The median eustachian foramen (=intertympanic foramen or median pharyngotympanic foramen) is large, circular, and incised into the ventral margin of the basioccipital. The basisphenoid forms the anterior margin of the foramen with a small part of the basioccipital-basisphenoid suture evident around the foramen (Figure 4).

The lateral aspect of the prootic is well exposed on the right side of MNA V2460. The outline of the prootic is that of a right triangle with a vertical posterior margin at the contact with the opisthotic, a horizontal ventral border at the contact with the basisphenoid, and a ventrally sloping anterior margin at the contact with the parietal, laterosphenoid, and quadrate. The prootic can be further divided into a deep braincase-forming surface and a more laterally placed flange, equivalent to the prootic-basisphenoid flange of Walker (1990). In the case of *E. colberti*, it is unclear if the basisphenoid formed much, if any, of the flange, so we will proceed with referring to this structure simply as the prootic flange. Posterior and deep to the flange, the prootic forms the anterior margin of the fenestra ovalis (Figure 6). Immediately anterior to the fenestra, the prootic is pierced by a foramen for the passage of cranial nerve VII. A groove extends dorsally from the foramen marking the course of the hyomandibular branch of the facial nerve. A shallow groove extends ventrally from the foramen as well, which we interpret as marking the course of the palatal branch of the facial nerve. Immediately posterior to this groove, a deep pneumatic depression is present as is seen in *S. acutus* (Walker, 1990, fig. 51) and *D. elaphros* (Wu & Chatterjee, 1993, fig. 7). Ventrally adjacent to the depression is the posterior most extent of the prootic/basisphenoid suture. The prootic/basisphenoid contact continues anteriorly in a straight line as the prootic sutures to the basisphenoid plate of the braincase. This suture terminates ventral to the trigeminal foramen.

Immediately anterior to the trigeminal foramen, the triple contact between the prootic, basisphenoid, and laterosphenoid is present but poorly preserved, making its characterization difficult. However, it would appear to have been anteroposteriorly longer than in crocodylomorph taxa such as *S. acutus* and *D. elaphros*. The trigeminal foramen is telescoped with the prootic forming the posteroventral margin of the spout-like opening. The space below and medial to the prootic flange is invaded by pneumatic sinuses, which Walker (1990) proposed calling the facial antrum. This pneumatic space is partitioned by bony struts arising from the deep surface of the prootic supporting the flange. Distinct cavities are present anterior and posterior to the "spout" of the trigeminal foramen (Walker, 1990: pg. 39). A particularly robust strut of bone (the prootic buttress) extends from the dorsal margin of the deep surface of the prootic to support the large quadrate facet located on the external surface of the prootic flange, and furthermore divide the facial antrum from the mastoid antrum behind (Figure 6a). As noted by Walker (1990) for *S. acutus*, it is along this buttress that we see the groove for the hyomandibular branch of the facial nerve.

It is unclear exactly what the external surface of the basisphenoid would look like in *E. colberti* because it appears much of its external surface is not preserved. Thus, this leaves unanswered whether this taxon would have possessed large basipterygoid processes as is plesiomorphic for Crocodylomorpha or a more plate-like external surface, as in protosuchids and other crocodyliforms (e.g., *P. richardsoni*, *O. stormbergi*). However, given the absence of anything that looks like a robust

FIGURE 6 Skull of the holotype of *Eopneumatosuchus colberti* (MNA V2460) in (a) right lateral, (b) right ventrolateral, and (c) right posteroventral views. (b) and (c) are digital surface models from the μCT scan data. ala, articulation for the lacrimal; cp, carotid pillar; cap, capitate process; cif, crista interfenestralis; ccr, cotylar crest; fo, fenestra ovalis; fr, frontal; gs, groove on the subcapsular process; ica, internal carotid artery; ls, laterosphenoid; ma, mastoid antrum; od, otoccipital diverticulum; oc, occipital condyle; pa, parietal; pb, prootic buttress; pf, prefrontal; posr, postcarotid recess; prer, precarotid recess; rs, rhomboid sinus; scp, subcapsular process; II, optic nerve; V, trigeminal nerve; VII, facial nerve

strut supporting a basipterygoid process and the presence of a plate-like bone contacting the laterosphenoid and prootic anteriorly, it is our view that it is likely *E. colberti* possessed the crocodyliform condition.

Crompton and Smith (1980) misidentified a number of the structures formed by the basisphenoid. In particular, they indicated a sella turcica and basisphenoid rostrum, which is far too posteriorly located (Crompton & Smith, 1980, fig. 11.5A). Based on this, they further misinterpreted two long bony processes on the ventral surface of the braincase as basipterygoid processes. This led Crompton and Smith (1980) to conclude that the internal carotid artery did not travel in a distinct canal (vidian canal) in *E. colberti*. Correctly placing the sella turcica more anteriorly (confirmed in the CT scans) clarifies much of the misidentified morphology. In particular, the "basipterygoid processes" of Crompton and Smith (1980, figs. 11.4 and 11.5) are instead the bony tubes transmitting the internal carotid artery towards the pituitary fossa (carotid pillars sensu Walker, 1990), the external surfaces of which are visible behind the fragments of bone identified as parts of the pterygoids by Crompton and Smith (1980). It would seem these bone fragments were identified as pterygoids in part because of their contact with what Crompton and Smith (1980) thought were basipterygoid processes. In light of the reinterpretation of this anatomy, it is our conclusion that these fragments are part of the basisphenoid at its contact with the laterosphenoid and prootic.

Due to the weathered external surface of the basisphenoid near the contact with the basioccipital, the highly pneumatized nature of the bone is evident. A large strut extends from the base of the otic capsule posteroventrally to the contact with the basioccipital. Moving medially from this strut, two smaller struts are present defining a series of interconnected recesses. This series of struts is mirrored on the other side of the skull. The recesses are confluent with the median eustachian system and communicate with the middle ear cavity. The lateralmost portion of this pneumatized space may be homologous with the rhomboid sinus of extant crocodylians (Figure 6; Colbert, 1946; Owen, 1850). Moving anteriorly, a bony process extends from the ventral margin of each otic capsule. These meet at the midline to form a slight process suspended from the braincase floor. This is the carotid pillar as is seen in *S. acutus* (Walker, 1990, fig. 23), *P. richardsoni* (Clark, 1986), and *P. haughtoni* (Busbey & Gow, 1984, fig. 8). Beginning at the internal opening of the internal carotid foramen, a groove is present running towards the subcapsular process at which point it descends towards the carotid pillar. There is a clear opening in the lateral surface of the pillar where the internal carotid and the palatal branch of the facial nerve would have entered into the vidian canal formed within the pillar (Figure 6). Extending ventrally off the carotid pillar near the aforementioned foramen is a small process that flattens ventrally and just meets its contralateral complement. A large space is present between the carotid pillar and the braincase floor, which Walker (1990) termed the postcarotid recess. The space ventral to the pillar is the precarotid recess. Both of these spaces communicate posteriorly with the median eustachian foramen.

The laterosphenoid has a vertical interdigitating suture with the prootic immediately dorsal to the trigeminal foramen. The bone sweeps forward with a horizontal contact with the overlying parietal bone. The capitate process is acute and underlies the postorbital process. The laterosphenoid forms the anterodorsal margin of the spout-shaped trigeminal foramen (Figures 4,6). Near the ventral margin of the laterosphenoid near the contact with the basisphenoid, a groove extends anteriorly from the trigeminal foramen that would have transmitted the ophthalmic division of the trigeminal nerve (V1). A bony ventral process arises from the laterosphenoid, which partially covers the V1 groove. We follow Crompton and Smith (1980) and Busbey and Gow (1984) in interpreting this as a partially ossified pila antotica. The anterior edge of the laterosphenoid is incised by a deep notch, which is presumably the result of the passage of the optic nerve in this area.

4.2 | Endocranial anatomy

High-resolution scans allow for the visualization and description of the endocranial cavity of *E. colberti* (Figure 7). Previous researchers noted that these casts reflect the general contours of the external surface of the endocranium, not the morphology of the brain itself (Kley et al., 2010). In both avians and crocodylians, however, 3D geometric morphometric studies demonstrate there is a strong correlation between these two elements and that analyses of endocranial casts likely closely reflect brain morphology (Watanabe et al., 2019).

Overall, the specimen is in remarkably good condition. We observe no significant distortion and the only part of the endocast that is missing is the anterior-most portion that would have been preserved in the snout, such as the nasal cavity (Pierce et al., 2017). The endocranial cast of *E. colberti* is cylindrical in shape, similar to that of other pseudosuchian archosaurs and close relatives (Bona et al., 2017; Kley et al., 2010; Lautenschlager & Butler, 2016; Leardi et al., 2020; Lessner & Stocker, 2017; Nesbitt et al., 2017; Pierce et al., 2017). When viewed laterally (Figure 7b), the dorsal aspect of the endocast is nearly straight, with only two minor depressions: one between the cerebrum and cerebellum and the other at the posterior abrupt step, which is less pronounced than that observed in

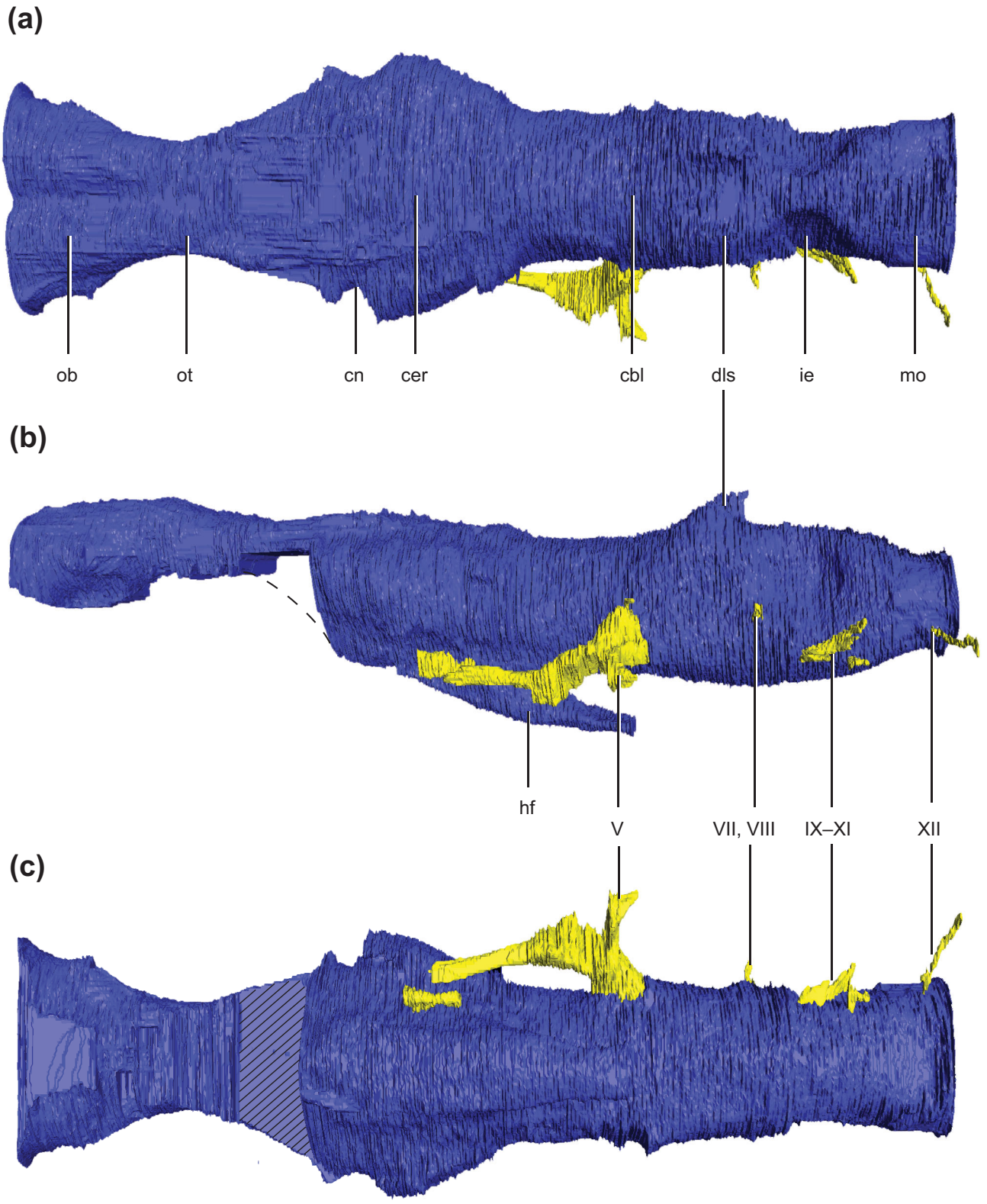

FIGURE 7 Digital reconstruction of the endocast of *Eopneumatosuchus colberti* (MNA V2460) in dorsal (a), left lateral (b), and ventral (c) views. Dashed line in (b) and hatching in (c) represent missing portions of endocast. cbl, cerebellum; cer, cerebrum; cn, cerebral notch; dls, dorsal branch of the longitudinal venous sinus; hf, hypophyseal (pituitary) fossa; ie, notch for the inner ear; mo, medulla oblongata; ob, olfactory bulb; ot, olfactory tract; V, endocast of trigeminal nerve; VII, VIII, endocast of facial and vestibulocochlear nerves; IX–XI, glossopharyngeal, vagus, and accessory nerve region; XII, hypoglossal nerve region

other crocodylomorphs (e.g., *Diplocynodon tormis, Lohuecosuchus megadontos*, *P. typus*). This condition most resembles the teleosaurid thalattosuchian *M. bollensis* and the noncrocodyliform crocodylomorph *A. figarii*, and contrasts with taxa that are characterized by a convex structure, such as *Simosuchus clarki* (Kley et al., 2010, fig. 32; Herrera et al., 2018, fig. 3; Leardi et al., 2020, fig. 11). Dorsally, the endocranial cast is nearly biconvex, with the cerebellum being the widest point, although the posteriormost aspect of the endocast is narrower than the olfactory region of the nasal cavity (Figure 7).

The olfactory region of the nasal cavity is nearly completely preserved, only missing the anteriormost aspect. This chamber is relatively large, being noticeably wider than the olfactory tract and nearly as broad as the cerebral hemispheres (Figure 7a). There is a deep, central groove in the olfactory region, which results in a distinct paired bulbous morphology. This resembles the condition observed in the metriorhynchoid thalattosuchian *P. typus* and the notosuchian *S. clarki* (Kley et al., 2010, fig. 32A; Pierce et al., 2017, fig 5). In contrast, this region is undivided in most other crocodylomorphs, regardless of phylogenetic position (Leardi et al., 2020). The olfactory tract is straight, relatively short, and undivided. This morphology is most similar to *A. figarii* and contrasts with that of many other sampled crocodyliforms, in which the olfactory tract is long and narrow (Herrera et al., 2013; Pierce et al., 2017; Serrano-Martínez et al., 2019, 2019b, 2020; Sertich & O'Connor, 2014).

The cerebrum of *E. colberti* is expanded in dorsal view and lacks separate expansions for cerebral hemispheres (Figure 7). This differs from the heart or spade-shaped morphology that characterizes *Anatosuchus minor*, *Araripesuchus wegeneri*, and *P. typus* (Sereno & Larsson, 2009, figs 10, 22; Pierce et al., 2017, fig. 5). Unlike any other sampled crocodylomorphs, there are shallow notches on the anterior portion of the lateral margins that are visible in dorsal view. In lateral view, the cerebrum is characterized by nearly flat dorsal and ventral margins, which differs from the dorsoventrally expanded endocranial cast of *A. figarii*, *Dip. tormis*, *P. typus*, *S. clarki*, and living crocodylians (Kley et al., 2010; Leardi et al., 2020; Pierce et al., 2017; Serrano-Martínez, Knoll, Narváez, & Ortega, 2019). In taxa that lack a groove between the cerebral hemispheres, a midline prominence has previously been associated with a dorsal dural venous sinus system, however *E. colberti* appears to lack both features (Kley et al., 2010).

The pituitary projects posteroventrally from the ventral margin of the endocast. The angle of this projection is acute, which is similar to the morphology of *Agaresuchus fontisensis*, *P. typus*, *S. clarki*, and *M. bollensis*, but differs from the nearly right angle of *A. figarii* and the near vertical orientation of the phytosaur *Parasuchus angustifrons* (Herrera et al., 2018; Lautenschlager & Butler, 2016; Leardi et al., 2020; Pierce et al., 2017; Serrano-Martínez et al., 2020). This feature is approximately half the width of the cerebrum, although it narrows slightly posteriorly, and extends to the anterior margin of the cerebellum. The morphology of the pituitary is most similar to that of the marine crocodylomorph *M. bollensis* but differs markedly from most other sampled crocodylomorphs in key aspects (Herrera et al., 2018, fig. 5). For example, the eusuchians *A. fontisensis*, *Dip. tormis*, and *L. megadontos* and the peirosaurid *Rukwasuchus yajabalijekundu* are characterized by more gracile and circular pituitaries, whereas the notosuchian *S. clarki* and especially the thalattosuchian *P. typus* exhibit a dorsoventrally expanded structure (Kley et al., 2010; Pierce et al., 2017; Serrano-Martínez et al., 2019, 2019b, 2020; Sertich & O'Connor, 2014).

The cerebellum, separated from the cerebrum by a dorsoventral and mediolateral constriction, is dorsoventrally expanded. The dorsal margin of the cerebellum is characterized by two prominent crests (Figure 7a,b). Similar structures were noted in aquatic crocodylomorphs, including a Chilean metriorhynchid *Plagiophthalmosuchus* ("*Steneosaurus*") cf. *gracilirostris* and *P. typus* and were identified as branches of the dorsal longitudinal venous sinus (Fernández et al., 2011, fig. 4; Brusatte et al., 2016, fig. 6; Pierce et al., 2017: fig. 5). Posterior to these structures are marked constrictions on either side of the cerebellum, resulting in an hourglass morphology of the dorsal margin (Figure 7a). The vestibular depression is also present in other examined crocodylomorphs, such as *A. figarii* and *S. acutus*, although it is more pronounced than the condition observed in *P. typus* (Leardi et al., 2020; Pierce et al., 2017; Walker, 1990).

In dorsal view, the medulla oblongata is cylindrical and shows no clear division with the cerebellum, however, in lateral view, this structure is dorsoventrally compressed (Figure 7b). When viewed posteriorly, this compression results in an oval cross-section. This minor flattening more closely resembles the condition displayed in sampled thalattosuchians (Brusatte et al., 2016; Herrera et al., 2018; Pierce et al., 2017). This condition differs from that of *A. figarii* and *S. acutus*, which exhibit a pronounced posterior abrupt step (Leardi et al., 2020).

4.3 | Endosseous labyrinth

The endosseous labyrinths of *E. colberti* are preserved well enough to allow for a general description and comparison of their anatomy to other crocodylomorphs (Figure 8). The anterior semicircular canal is dorsoventrally taller than the posterior semicircular canal. This morphology is similar to that of other terrestrial and semiaquatic

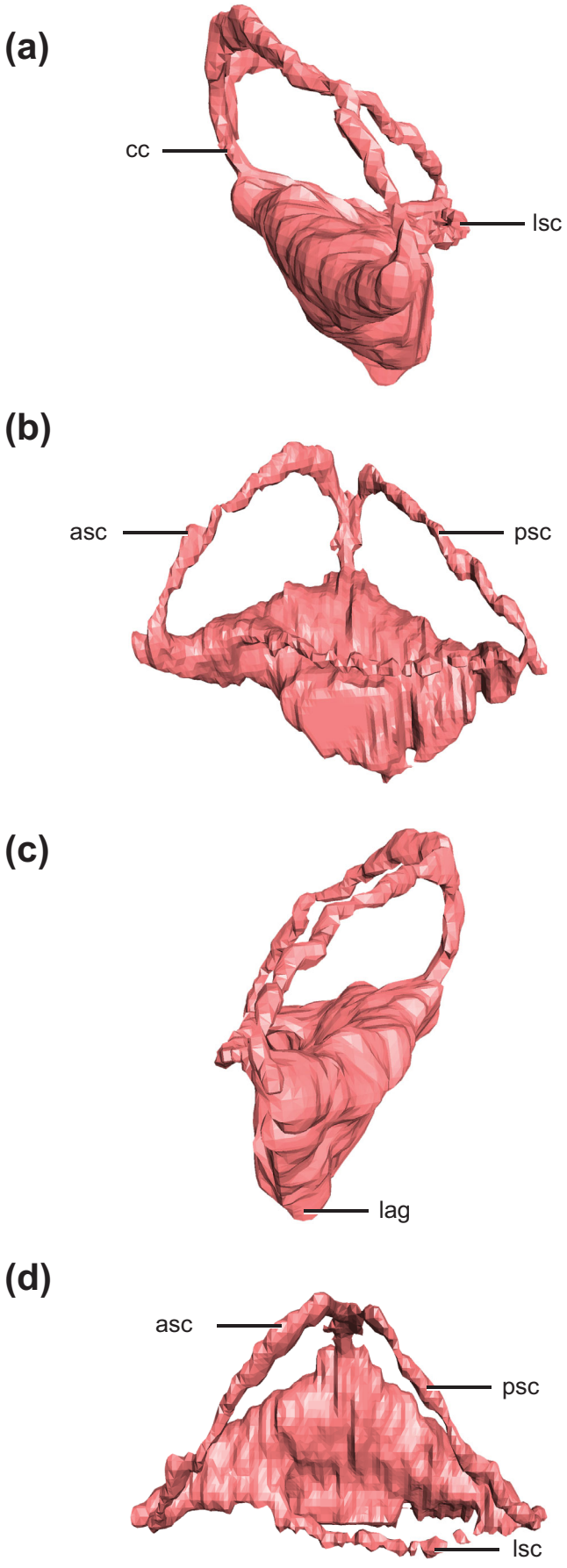

crocodylomorphs, although the canals are of equal height in *A. figarii* (Leardi et al., 2020; Schwab et al., 2020), and dissimilar to avemetatarsalians that have more prominent anterior semicircular canal (Bronzati et al., 2021). The straight line anteroposterior length of these two canals is nearly equal. The common crus is relatively narrow in lateral and anterior views, being approximately three times tall as it is wide. Terrestrial early crocodylomorphs and semiaquatic thalattosuchians also have a narrow common crus, whereas those thalattosuchians hypothesized to be pelagic and extant crocodylians exhibit a much more robust structure (Schwab et al., 2020). The lateral semicircular canal is nearly straight in dorsal view and is the narrowest and shortest in length of the three structures, which is also the case in other sampled crocodylomorphs (Bronzati et al., 2021; Brusatte et al., 2016; Herrera et al., 2018; Kley et al., 2010; Leardi et al., 2020; Schwab et al., 2020; Serrano-Martínez, Knoll, Narváez, Lautenschlager, & Ortega, 2019). All three semicircular canals have relatively thin cross-sections (Figure 8), a common feature of terrestrial and semiaquatic crocodylomorphs, which are characterized by relatively tall skulls compared to more aquatic relatives (Bronzati et al., 2021; Schwab et al., 2020). The lagena has a moderate length, falling between the extremes of *J. sloani* and *P. haughtoni* (tall) and that of *Cricosaurus araucanensis* and *C. schroederi* (short) (Herrera et al., 2018; Schwab et al., 2020). Unlike living crocodylians, the lagena is nearly straight (Brusatte et al., 2016; Pierce et al., 2017).

4.4 | Cranial pneumaticity

CT scans reveal previously unreported aspects of the pneumatic cavities of *E. colberti*. In general, these scans demonstrate the remarkable extent to which pneumaticity permeates the preserved skull of *E. colberti* (Figure 9). Together, these cavities surround much of the endocranial cast and imbue nearly every element of the braincase, representing a potential extreme in the crocodylomorph clade.

The posterior aspect of the paired frontals exhibits a distinct anterodorsally projecting sinus that is adjacent to the cerebrum. This pneumatic cavity continues into the dorsalmost aspects of the laterosphenoid. These pneumatic chambers are between the endocranial cast and the supratemporal fenestrae and appear to be the trigeminal recess described in detail by Leardi et al. (2020). These

FIGURE 8 Left semicircular canals of *Eopneumatosuchus colberti* (MNA V2460) reconstructed using CT data in (a) anterior, (b) left lateral, (c) posterior, and (d) dorsal view. asc, anterior semicircular canal; cc, common crus; lag, lagena; lsc, lateral semicircular canal; psc, posterior semicircular canal

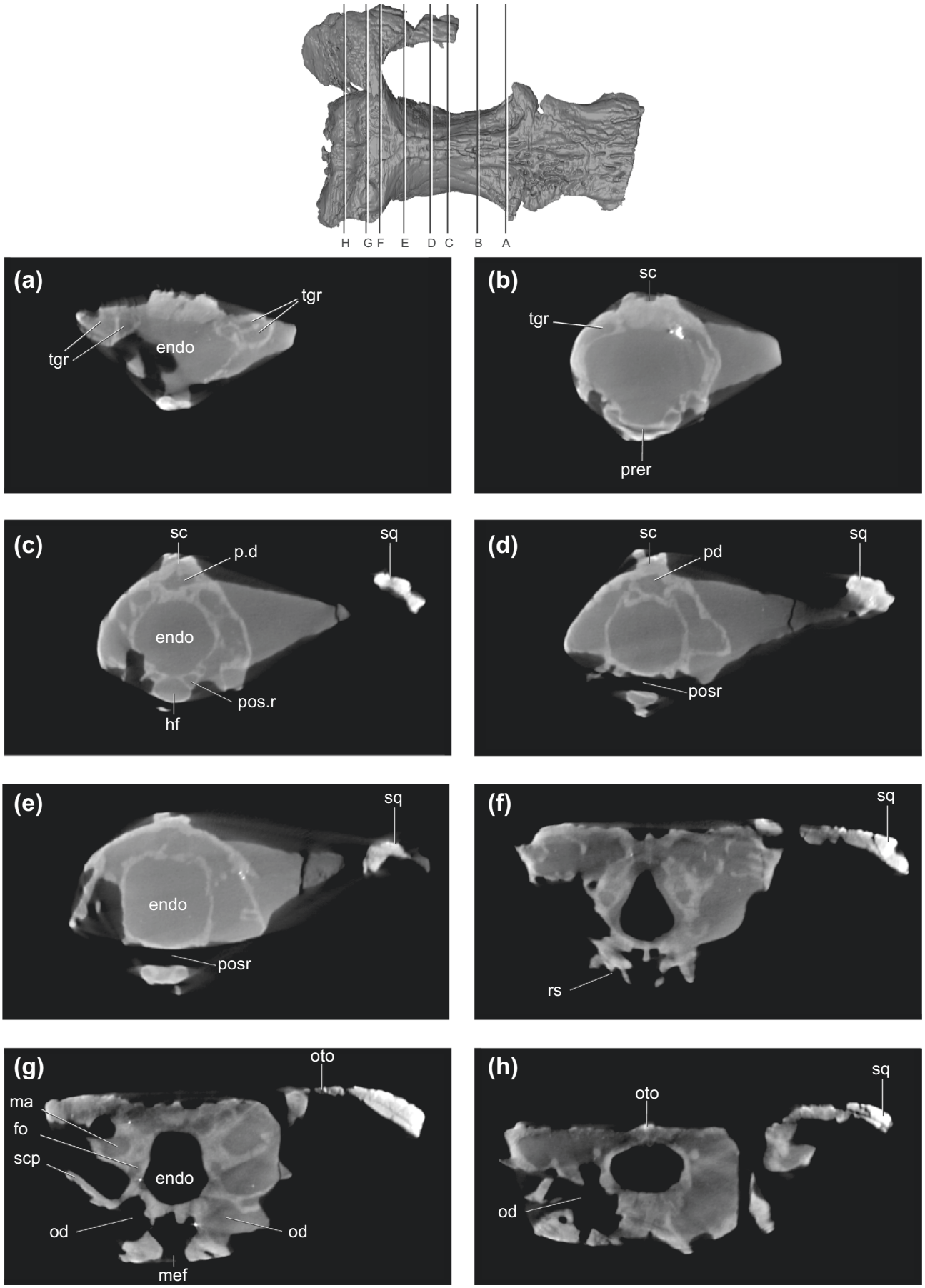

FIGURE 9 Legend on next page.

structures are similar to those of *A. figarii* in that they bifurcate anteriorly; however, they differ in that the recesses extend anteriorly to a greater degree (Figure 9a; Leardi et al., 2020). Posteriorly, this pneumatization extends dorsally and medially, resulting in extensive paired hollow chambers that border the endocast and a significantly wider laterosphenoid than observed in *A. figarii*.

Ventrally, the basisphenoid is extensively pneumatized and characterized by a number of distinct chambers (Figure 6). The majority of the precarotid recess has been lost, with only a small anterior section remaining (Figure 9b). The preserved precarotid recess is dorsoventrally low and mediolaterally wide and underlies the pituitary anteriorly. The morphology of this structure, however, is likely influenced by minor crushing that has reduced the dorsoventral height of the chamber. Posteriorly, this cavity would continue on the posterior portion of the basisphenoid, but the ventral margin is no longer present (Figures 6 and 9). The postcarotid recess overlies the carotid pillar, including the hypophyseal fossa and internal carotid arteries (Figures 6 and 9c–e). Anteriorly, this recess is divided and originates along the dorsolateral margin of the pituitary fossa (Figure 9c). The two diverticula increase in size posteriorly and merge to become a single large pneumatic chamber, which is open laterally and was cleaned of sediment during original preparation. When viewed laterally, the postcarotid recess is semicircular in shape, with the dorsal margin nearly flat. It is dorsoventrally taller than that of *P. haughtoni* (Busbey & Gow, 1984, fig. 8).

The anterior portion of the sagittal crest lacks pneumaticity, creating a marked contrast between the chambers that characterize the laterosphenoid at this same point (Figure 9b). Near the midpoint of the parietal, nearly in line with the anterior extent of the squamosal and contact with the prootic, a central pneumatic chamber appears, which increases in size posteriorly (Figure 9c,d). This chamber widens to eventually create another pneumatic cavity above the endocranial cast, which is absent in *A. figarii* but is present in extant *Alligator* (i.e., parietal diverticulum) (Dufeau & Witmer, 2015). The lateral trigeminal recesses amalgamate with this central chamber near the posterior margin of the parietal, creating a large pneumatic region that surrounds the endocranial cavity (Figure 9e).

These pneumatic chambers continue and expand posteriorly, creating an extensive and complex set of interconnected chambers that imbue the posterior portion of the braincase (Figure 9e–h). In particular, this internal chamber permeates the prootic, otoccipital, basioccipital, and potentially the supraoccipital. This contrasts with the other early branching crocodylomorph with well-documented internal pneumaticity, *A. figarii*, which exhibits discrete pneumatic diverticula (Leardi et al., 2020: fig. 13). The extent of interconnectedness resembles that of *P. haughtoni*, in which the fenestra ovalis and otic capsule are linked dorsally by the fenestra pseudorotunda, and ventrally the lateral pharyngotympanic canal, ventral pneumatic sinus, and rhomboid sinus all interconnect (Busbey & Gow, 1984). In *E. colberti*, the extensive cavity represents the amalgamation of the intertympanic diverticulum (the "mastoid antrum" of Clark, 1994 and Leardi et al., 2020), rhomboid sinus, and otoccipital diverticulum (posterior tympanic recess of Wu & Chatterjee, 1993; Figure 9f,g). The extent of cranial pneumaticity differs dramatically from that of thalattosuchians, in which the pneumatic cavities are reduced in the braincase and limited in the quadrates (Herrera et al., 2018; Leardi et al., 2020; Pierce et al., 2017). Unfortunately, the quadrates of *E. colberti* are not preserved. In many noncrocodyliform crocodylomorphs, this structure are extensively pneumatized, including *A. figarii*, *D. elaphros*, and *Macelognathus vagans* (Leardi et al., 2017; Leardi et al., 2020; Wu & Chatterjee, 1993).

5 | DISCUSSION

5.1 | Phylogenetic relationships

Our phylogenetic analysis resulted in four most parsimonious trees of 1,748 steps (CI = 0.3124, RI = 0.7477). The strict consensus of these four trees is shown in Figure 10. The basic interrelationships of the major clades of crocodylomorphs are the same as in previous analyses of this matrix (Wilberg, 2015; Wilberg et al., 2019), with Thalattosuchia as the sister taxon of Crocodyliformes, and a basal dichotomy among Crocodyliformes between a large clade of early crocodyliforms ("protosuchians," gobiosuchids, shartegosuchids, and *Hsisosuchus*) and Mesoeucrocodylia (Figure 10). *Eopneumatosuchus colberti* is recovered as a member of Protosuchidae within this large early crocodyliform clade, sister taxon to *Protosuchus richardsoni* + *Orthosuchus stormbergi*. Given that some recent phylogenetic analyses have recovered *E. colberti* as the sister to Thalattosuchia (see Foffa et al., 2019; Johnson et al., 2020; Ősi et al., 2018; Sachs et al., 2019; Schwab et al., 2020), we tested this alternative phylogenetic

FIGURE 9 Select μCT through the skull of *Eopneumatosuchus colberti* (MNA V2460). The slice location of each panel (a–h) is indicated on the top digital surface model. endo, endocranial cavity; fo, fenestra ovalis; hf, hypophyseal (pituitary) fossa; ma, mastoid antrum mef, median eustachian foramen; od, otoccipital diverticulum; oto, otoccipital; pd, parietal diverticulum; posr, postcarotid recess; prer, precarotid recess; rs, rhomboid sinus; sc, sagittal crest; scp, subcapsular process; sq, squamosal; tgr, trigeminal recess

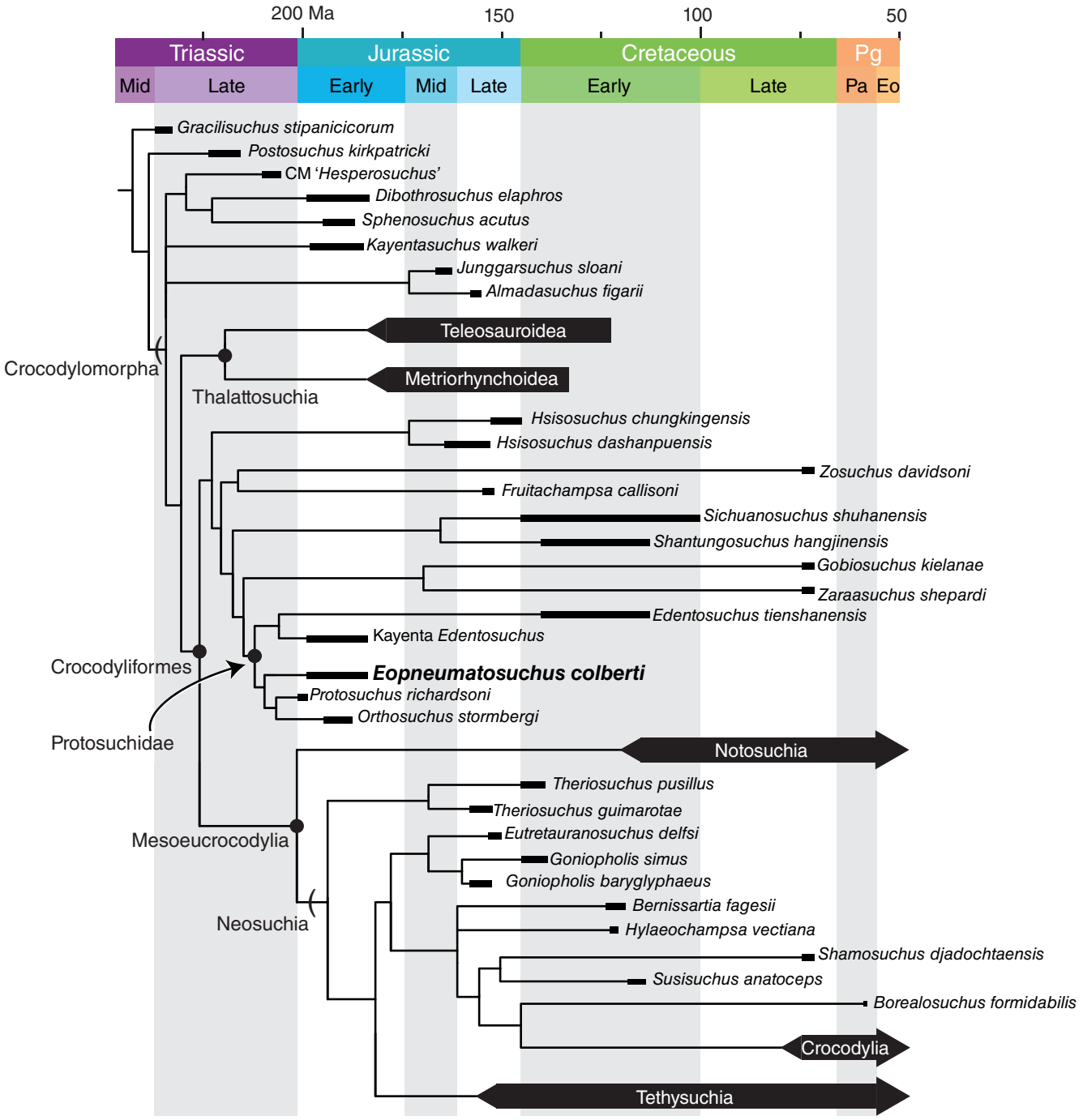

FIGURE 10 Time-calibrated phylogenetic hypothesis (strict consensus) of *Eopneumatosuchus colberti* (bold) and other early crocodylomorphs. Narrow bars represent the geologic uncertainty for a taxon's age range, whereas the thick bars for collapsed clades represent observed stratigraphic range. Circles at nodes indicate node-based clades, whereas arcs denote stem-based clades. Eo, Eocene; Mid, Middle; Pa, Paleocene; Pg, Paleogene

hypothesis by constraining it to be a member of a monophyletic Thalattosuchia. This constraint analysis demonstrates that it takes additional eight steps to place *E. colberti* as sister to Thalattosuchia. Additionally, this placement has no effect on thalattosuchian ingroup relationships.

The most parsimonious placement of *E. colberti* within Protosuchidae is supported by synapomorphies at each node. Among the 21 synapomorphies supporting the large clade of early crocodyliforms ("protosuchians," gobiosuchids, shartegosuchids, and *Hsisosuchus*), one is preserved in *E. colberti*: a descending process of the prefrontal that does not reach the palate (character 91, state 0). Protosuchids, gobiosuchids, and *Shantungosuchus hangjinensis* + *Sichuanosuchus shuhanensis* are united

by 11 synapomorphies, of which a single state is preserved in *E. colberti*: an open interfrontal suture (character 111, state 0). Protosuchidae is diagnosed by 11 synapomorphies, three of which are present in *E. colberti*: width of the cranial table is narrower than the ventral portion of the skull (character 56, state 1); posterior surface of the basioccipital ventral to the occipital condyle is short and gently curved (character 220, state 0); and a laterally open cranioquadrate canal (character 241, state 0). Finally, *E. colberti* is united in a clade with *P. richardsoni* + *O. stormbergi* diagnosed by four synapomorphies of which two are present in *E. colberti*: frontal and parietal ornamented by circular/subpolygonal pits (character 51, state 2); and a short, poorly developed squamosal prong (character 78, state 0).

These results demonstrate that although the dorsal skull table of *E. colberti* shares a number of apomorphies with thalattosuchians, there are numerous other character states, particularly in the basicranium, that it shares with protosuchids and other early crocodyliforms to the exclusion of thalattosuchians. Additionally, the extreme pneumatization of the braincase most resembles that of *P. haughtoni* (Busbey & Gow, 1984; Gow, 2000), and stands in stark contrast with the apneumatic condition observed in thalattosuchians (e.g., Herrera et al., 2018; Leardi et al., 2020; Pierce et al., 2017). Thus, these skull table character states (e.g., relatively wide interorbital region at nasal-frontal suture, large supratemporal fenestrae) appear to have evolved independently in *E. colberti* and thalattosuchians, which is not surprising because they also evolved separately in some tethysuchians.

Our topology differs, in part, from other recent investigations of early crocodyliform relationships in several notable aspects. The recovery of a close relationship between *P. richardsoni* and *O. stormbergi* contrasts with the results of Leardi et al. (2017) and Martínez et al. (2019), in which *O. stormbergi* is found outside Protosuchidae. The analysis of Buscalioni (2017), however, finds *O. stormbergi* within Protosuchidae but more closely related to *Edentosuchus tienshanensis* and the *Edentosuchus*-like taxon from the Kayenta Formation. Similarly, we find that both gobiosuchids and shartegosuchids to be more closely related to Protosuchidae than mesoeucrocodylians, which contrasts with the results these previous studies but is in line with the results of Wilberg (2015), which is the dataset on which the present analysis is based (Figure 10).

5.2 | Early evolution of the crocodylomorph endocranium

The internal anatomy of the pseudosuchian cranium, and for crocodylomorphs in particular, has become increasingly well-documented in recent years, although sampled taxa remain biased towards thalattosuchians and eusuchians, with a limited sampling of early crocodylomorphs (Bona et al., 2017; Bronzati et al., 2021; Brusatte et al., 2016; Erb & Turner, 2021; Herrera et al., 2018; Holliday et al., 2020; Holloway et al., 2013; Kley et al., 2010; Lautenschlager & Butler, 2016; Leardi et al., 2020; Lessner & Stocker, 2017; Nesbitt et al., 2017; Pierce et al., 2017; Serrano-Martínez et al., 2019, 2019b, 2020; Sertich & O'Connor, 2014; Stocker et al., 2016). The endocranial morphology of the earliest crocodylomorphs remains unknown, hindering our understanding of the major structural changes that occurred during early crocodylomorph evolution. Currently, endocranial casts are only known from two "sphenosuchian" crocodylomorphs, *S. acutus* and *A. figarii*, of which only the latter is completely described and digitally imaged (Leardi et al., 2020; Walker, 1990). Relative to early archosauriforms such as phytosaurs, ornithosuchids, and aetosaurs, early crocodylomorphs exhibited a relatively low and straight endocast with a short olfactory tract in lateral view (Lautenschlager & Butler, 2016; Baczko & Desojo, 2016; Lessner & Stocker, 2017; Baczko et al., 2016). Additionally, the olfactory bulbs are not paired and there is a well-defined posterior abrupt step posterior to the cerebellum. Unfortunately, how widespread these traits are among other non-crocodyliform crocodylomorphs remains unknown given such limited sampling.

The endocranial cast of *E. colberti* is most similar to that of both *A. figarii*, a noncrocodyliform crocodylomorph from the Late Jurassic, and those of Early Jurassic thalattosuchian crocodylomorphs (Brusatte et al., 2016; Herrera et al., 2018; Leardi et al., 2020; Pierce et al., 2017), providing insights into endocranial morphology among ancestral crocodylomorphs. In particular, these taxa all exhibit low, straight endocasts, which differ from the morphologies of early archosauriforms and later mesoeucrocodylians. Thalattosuchians and *E. colberti* share a notable dorsal longitudinal venous sinus (Pierce et al., 2017), which is not observed in *A. figarii* (Leardi et al., 2020). Therefore, this feature may have evolved once in the common ancestor of thalattosuchians and *E. colberti* and then was subsequently lost in other crocodylomorphs, or evolved independently multiple times. Overall, the limited available sampling suggests the general tubular shape of the endocranium remained relatively stable early in crocodylomorph evolution.

The endocranial morphology of *E. colberti* also sheds light on a key morphological transition in cerebral hemisphere shape at or near the origin of Crocodyliformes. In phytosaurs, *A. figarii*, and thalattosuchians these structures are nearly anteroposteriorly symmetrical in dorsal view (Herrera et al., 2018; Lautenschlager & Butler, 2016; Leardi

et al., 2020; Pierce et al., 2017), whereas in mesoeucrocodylians this feature is asymmetrical (e.g., Kley et al., 2010; Serrano-Martínez et al., 2019, 2019b). The asymmetrical nature of the cerebrum of *E. colberti*, with the prominent notch on its anterior margin (Figure 7), suggests that this trait was present by at least the common ancestor of all Crocodyliformes. The size of this notch, however, is unique to *E. colberti* among the endocrania of described crocodylomorphs. *Eopneumatosuchus colberti* also exhibits a prominent groove separating its olfactory bulbs, which is a feature shared with both thalattosuchians and the notosuchians *Simosuchus clarki* and *Campinasuchus dinizi* (Fonseca et al., 2020; Kley et al., 2010; Pierce et al., 2017). Divided olfactory bulbs are also found in at least one phytosaur, *Parasuchus angustifrons* (Lautenschlager & Butler, 2016: fig. 2) and one early suchian, *Parringtonia gracilis* (Nesbitt et al., 2017: fig. 11), although the groove observed in both taxa is less pronounced than that observed in *E. colberti*. The presence of a medial sulcus dividing the olfactory bulbs appears to be a relatively variable trait, because this feature is not present in other sampled phytosaurs (e.g., *Ebrachosuchus neukami*) and crocodylomorphs (e.g., *A. figarii* or later eusuchians). This pattern may suggest that divided olfactory bulbs either independently evolved throughout archosauriforms, including near the base of Crocodyliformes where it was lost before the evolution of Eusuchia, or evolved a single time near the base of Crurotarsans and was lost repeatedly.

The shape of the endocranium of *E. colberti* constrains the appearance of a curved endocranial dorsal margin to after the evolution of protosuchians. The relatively straight dorsal margin exhibited by early crocodylomorphs differs from the curved endocranium that characterizes notosuchians and eusuchians (Fonseca et al., 2020; Kley et al., 2010; Serrano-Martínez et al., 2019, 2019b, 2020; Sertich & O'Connor, 2014). Additionally, it provides further evidence that the elongate olfactory tract, which is likely linked to snout length, appeared independently in thalattosuchians and mesoeucrocodylians, because it is absent in *E. colberti*. Although *E. colberti* fills some key gaps in our understanding of early crocodylomorph endocranial evolution, the real picture is no doubt more complex, emphasizing the importance of sampling additional early crocodyliform endocrania. In particular, it would be helpful to constrain the timing and phylogenetic position of the development of the endocast flexure that characterizes many mesoeucrocodylians.

In comparison to later crocodyliforms, *E. colberti* displays significant differences in olfactory bulb and tract lengths, widths, heights, and the degree to which they are divided. For example, sampled eusuchians, such as *Diplocynodon tormis* and *Lohuecosuchus megadontos*, exhibit tubular olfactory bulbs and narrow olfactory tracts, which contrasts with the wide morphology of both of these structures in *E. colberti* (Serrano-Martínez et al., 2019, 2019b, 2020). Additionally, in all eusuchians the olfactory tract is significantly longer (Serrano-Martínez et al., 2020). Eusuchians, including living taxa, also exhibit a noteworthy dorsoventral compression of the hindbrain as well as a marked ventral displacement (Bona et al., 2017; Pierce et al., 2017; Serrano-Martínez et al., 2019, 2019b, 2020). Although the ventral displacement differs dramatically, a slightly wider than long hindbrain is also observed in *E. colberti*. In sum, the wide range of morphologies, even among closely related taxa, suggests that this region is notably less conservative than previously suggested.

5.3 | Implications for early crocodyliform paleoecology

It has previously been hypothesized that the end-Triassic mass extinction acted as a trigger for the diversification of the surviving crocodylomorphs (Toljagic & Butler, 2013). For example, the loss of the carnivorous, semiaquatic phytosaurs and the herbivorous, terrestrial aetosaurs opened novel ecological roles for the surviving crocodylomorph clade (Stubbs et al., 2013). The Kayenta Formation preserves a remarkable diversity of crocodylomorphs consistent with this hypothesis. Crocodylomorph taxa known from the Kayenta Formation include *C. valliceps*, *E. colberti*, *Kayentasuchus walkeri*, and two unnamed *Edentosuchus*-like taxa. *Protosuchus richardsoni* was recovered from the Lower Jurassic Moenave Formation of the same area (Colbert & Mook, 1951). These taxa exhibit a marked ecological disparity. *Protosuchus richardsoni*, known from multiple, well-preserved skeletons was likely terrestrial—inferred from relatively long, gracile limbs (Wilberg et al., 2019). Additionally, this habitat is likely shared by the closely related *Edentosuchus*-like taxa. Although only known from a skull, *Edentosuchus tienshanensis* from the Lower Cretaceous of China, was found at the same locality as a set of articulated vertebrae and partial hindlimb (GMPKU-P 200102), which both exhibit characters that strongly suggest a terrestrial habit (Pol et al., 2004). Thus, given that *P. richardsoni* and *Ed. tienshanensis* were likely terrestrial, it is probable that the *Edentosuchus*-like taxa were as well. *C. valliceps* is characterized by a narrow and elongate snout, which strongly resembles that of living crocodylians (Tykoski et al., 2002). This resemblance may suggest a semiaquatic ecological role, the first record of an ecology that characterizes all living representatives of this clade (Grigg & Kirshner, 2015), and could illustrate the occupation of novel habitats with the loss of phytosaurs during the end-Triassic mass extinction; however, the absence of limb material and its placement

among either other terrestrial crocodyliforms or semiaquatic goniopholids makes a precise reconstruction equivocal (Wilberg et al., 2019). In addition to a potential increase in habitat diversity, there are intriguing hints of new diets. In particular, analyses of phenotypic dental complexity demonstrate exceptionally high tooth complexities in two undescribed early crocodyliforms that strongly suggest herbivory (Melstrom & Irmis, 2019).

The recovery of *E. colberti* as a protosuchid increases the known diversity of the group during the Early Jurassic, reinforcing the hypothesis that this clade rapidly diversified following the end-Triassic mass extinction, but also complicates our understanding of the development of early crocodylomorph ecology. Some recent phylogenetic work has recovered this taxon within Thalattosuchia, which is a clade characterized by a marine habitat and multiple adaptations for a pelagic lifestyle (Johnson et al., 2020; Wilberg et al., 2019), or just outside Thalattosuchia. Reconstructions of habitat transitions have found a rapid shift from terrestrial directly to marine environments in Thalattosuchia (Wilberg et al., 2019). Unlike other transitions to marine habitats in the crocodylomorph clade, there is no recorded intermediate shift to freshwater habitats. The depositional environment of the Kayenta Formation, a fluvial system far away from marine sediments, precludes a fully pelagic lifestyle of *E. colberti*. Inner ear morphology may provide additional habitat evidence. Three dimensional geometric morphometric studies of semicircular canals recovered *E. colberti* in an intermediate position with regard to other crocodylomorphs. In a plot of PC1 versus PC2 morphospace, MNA V2460 plotted closest to terrestrial taxa (i.e., *P. haughtoni*, *Junggarsuchus sloani*), though it occupies its own disparate part of morphospace (Schwab et al., 2020). In contrast, PC1 vs. PC3 and canonical variate morphospace plots show *E. colberti* with semiaquatic taxa, suggesting a semiaquatic lifestyle (Schwab et al., 2020). As the earliest branching thalattosuchian, *E. colberti* filled a key paleoecological gap and may have represented the rapid intermediate step between terrestrial crocodylomorphs and marine thalattosuchians.

As a protosuchid, however, the inference of a semiaquatic habitat may be less certain. The grouping with other terrestrial crocodylomorphs in PC1 versus PC2 plots of semicircular canal morphospace may suggest a terrestrial habit (Schwab et al., 2020). A terrestrial lifestyle would also be consistent with a braincase pneumatized to the extent observed in *E. colberti*. Other early crocodylomorphs and protosuchids that possess pneumatized braincases are terrestrial taxa, whereas marine crocodylomorphs typically exhibit a marked reduction in pneumaticity, although this may also be related to phylogenetic relationships (Herrera et al., 2018). When an alternative phylogenetic hypothesis was investigated, in which *E. colberti* was the sister taxon to Thalattosuchia + (*Shamosuchus djadochtaensis* + Crocodylia), habitat reconstructions changed little (Schwab et al., 2020). The placement of *E. colberti* as a sister taxon to *P. haughtoni* was not tested. The reconstruction of habitat using morphology of the inner ear has also recently been called into question by a broad investigation of archosaur semicircular canal morphology, which found no significant relationship between labyrinth shape and habitat transition and instead found that shape is associated with the broad dimensions of the posterior skull (Bronzati et al., 2021). In this case, the inner ear morphology of *E. colberti* may be explained by the relatively flat skull. If, however, the shape of the inner ear indicates habitat and both a semiaquatic habit and its placement as a protosuchian continue to be supported, *E. colberti* may represent a second possible transition into this environment, independent of *C. vasliceps*. We view this as less likely than the alternative, which is a terrestrial lifestyle like that inferred for other protosuchids.

6 | CONCLUSIONS

Here, we redescribed the cranial morphology, examined endocranial anatomy, and evaluated the phylogenetic relationships of the Early Jurassic taxon *Eopneumatosuchus colberti*. We noted some differences from the original description of Crompton and Smith (1980), especially in the morphology of the back of the skull and cranial pneumaticity. A phylogenetic analysis recovered *E. colberti* as the sister taxon to *Protosuchus richardsoni* and *Orthosuchus stormbergi*, which expanded the diversity of protosuchids during the Early Jurassic. Computed tomography of internal anatomy demonstrated striking similarities to that of *Almadasuchus figarii*, a noncrocodyliform crocodylomorph, and *Macrospondylus bollensis*, a thalattosuchian; but *E. colberti* also shared some characteristics with other crocodyliforms. Crocodylomorph endocranial anatomy may be more variable than previously suggested. *Eopneumatosuchus colberti* represented a probable extreme in braincase pneumaticity within the crocodyliform clade, although the closely related *P. haughtoni* displayed many of the same pneumatic features. Computed tomography scans demonstrated pneumatic cavities that permeate all braincase elements and the interconnectedness of these chambers, which differs from the discrete foramina of *A. figarii*. Aspects of internal anatomy, such as the inner ear, displayed similarities with both terrestrial and semiaquatic crocodylomorphs, making ecological reconstructions of this taxon difficult until additional material is discovered.

ACKNOWLEDGEMENTS

Janet Gillette (MNA) kindly loaned the specimen for μCT scanning and study, and Larkin McCormack (MNA) provided additional information on the type locality. We

thank Samer Merchant (Preclinical Imaging, University of Utah) for producing the μCT scans of the specimen. Adam Marsh (Petrified Forest National Park) provided valuable additional information and discussion on the geology and stratigraphic position of the type locality. We are extremely grateful for the constructive comments provided by two reviewers, which resulted in a significantly improved manuscript. Juan Martín Leardi and Stephanie Abramowicz helpfully provided photos of *Orthosuchus stormbergi* and *Fruitachampsa callisoni*, respectively. Funding was provided by an NSF Graduate Research Fellowship (KMM), NSF DEB 1257485 and NSF DEB 1754596 (AHT), and the University of Utah (RBI).

AUTHOR CONTRIBUTIONS

Keegan Melstrom: Conceptualization (equal); data curation (lead); formal analysis (equal); funding acquisition (supporting); investigation (equal); methodology (equal); project administration (lead); resources (supporting); software (supporting); supervision (lead); validation (equal); visualization (equal); writing – original draft (lead); writing – review and editing (lead). **Alan Turner:** Formal analysis (equal); funding acquisition (equal); investigation (equal); methodology (equal); resources (equal); software (equal); visualization (equal); writing – original draft (supporting); writing – review and editing (supporting). **Randall Irmis:** Conceptualization (equal); data curation (supporting); formal analysis (supporting); funding acquisition (equal); investigation (supporting); methodology (supporting); project administration (supporting); writing – original draft (supporting); writing – review and editing (supporting).

ORCID

Keegan M. Melstrom https://orcid.org/0000-0002-6313-6146

REFERENCES

Baczko, M. B. v., & Desojo, J. B. (2016). Cranial anatomy and palaeoneurology of the archosaur *Riojasuchus tenuisceps* from the Los Colorados Formation, La Rioja, Argentina. *PLoS One*, *11*, e0148575.

Baczko, M. B. v., Taborda, J. R. A., & Desojo, J. B. (2018). Paleoneuroanatomy of the aetosaur *Neoaetosauroides engaeus* (Archosauria: Pseudosuchia) and its paleobiological implications among archosauriforms. *PeerJ*, *6*, e5456.

Bazard, D. R., & Butler, R. F. (1991). Paleomagnetism of the Chinle and Kayenta formations, New Mexico and Arizona. *Journal of Geophysical Research B*, *96*, 9847–9871.

Benton, M. J., & Clark, J. M. (1988). Archosaur phylogeny and the relationships of the Crocodylia. In M. J. Benton (Ed.), *The phylogeny and classification of the Tetrapods, volume 1: Amphibians, reptiles, birds* (pp. 295–338). Oxford, England: Clarendon Press.

Bona, P., Paulina Carabajal, A., & Gasparini, Z. (2017). Neuroanatomy of *Gryposuchus neogaeus* (Crocodylia, Gavialoidea): A first integral description of the braincase and endocranial morphological variation in extinct and extant gavialoids. *Earth and Environmental Science Transactions of the Royal Society of Edinburgh*, *106*, 235–246.

Breeden, B. T., III, & Rowe, T. B. (2020). New specimens of *Scutellosaurus lawleri* Colbert, 1981, from the Lower Jurassic Kayenta Formation in Arizona elucidate the early evolution of thyreophoran dinosaurs. *Journal of Vertebrate Paleontology*, *40*, e1791894.

Bronzati, M., Benson, R. B. J., Evers, S. W., Ezcurra, M. D., Cabreira, S. F., Choiniere, J., ... Nesbitt, S. J. (2021). Deep evolutionary diversification of semicircular canals in archosaurs. *Current Biology*, *31*, 2520–2529.

Bronzati, M., Montefeltro, F. C., & Langer, M. C. (2012). A species-level supertree of Crocodyliformes. *Historical Biology*, *24*, 598–606.

Bronzati, M., Montefeltro, F. C., & Langer, M. C. (2015). Diversification events and the effects of mass extinctions on Crocodyliformes evolutionary history. *Royal Society Open Science*, *2*, 140385.

Brown, B. (1934). A change of names. *Science*, *79*, 80.

Brusatte, S. L., Muir, A., Young, M. T., Walsh, S., Steel, L., & Witmer, L. M. (2016). The braincase and neurosensory anatomy of an early Jurassic marine crocodylomorph: Implications for crocodylian sinus evolution and sensory transitions. *Anatomical Record*, *299*, 1511–1530.

Busbey, A. B., III, & Gow, C. (1984). A new protosuchian crocodile from the Upper Triassic Elliot Formation of South Africa. *Palaeontologia Africana*, *25*, 127–149.

Buscalioni, Á. D. (2017). The Gobiosuchidae in the early evolution of Crocodyliformes. *Journal of Vertebrate Paleontology*, *37*, e1324459.

Clark, J. M. (1986). *Phylogenetic relationships of the crocodylomorph archosaurs* (Ph.D. dissertation), The University of Chicago, Chicago, IL.

Clark, J. M. (1994). Patterns of evolution in Mesozoic Crocodyliformes. In N. C. Fraser & H.-D. Sues H-D (Eds.), *In the shadow of the dinosaurs: Early Mesozoic tetrapods* (pp. 84–97). Cambridge: Cambridge University Press.

Clark, J. M. (2011). A new shartegosuchid crocodyliform from the Upper Jurassic Morrison Formation of western Colorado. *Zoological Journal of the Linnean Society*, *163*, 152–172.

Clark, J. M., & Fastovsky, D. E. (1986). Vertebrate biostratigraphy of the Glen Canyon Group in northern Arizona. In K. Padian (Ed.), *The beginning of the age of dinosaurs: Faunal change across the Triassic–Jurassic boundary* (pp. 285–301). Cambridge, MA: Cambridge University Press.

Clark, J. M., & Sues, H. D. (2002). Two new basal crocodylomorph archosaurs from the Lower Jurassic and the monophyly of the Sphenosuchia. *Zoological Journal of the Linnean Society*, *136*, 77–95.

Clark, J. M., Xu, X., Forster, C. A., & Wang, Y. (2004). A Middle Jurassic "sphenosuchian" from China and the origin of the crocodylian skull. *Nature*, *430*, 1021–1024.

Coddington, J. A., & Scharff, N. (1994). Problems with zero-length branches. *Cladistics*, *10*, 415–423.

Colbert, E. H. (1946). *Sebecus*, representative of a peculiar suborder of fossil Crocodilia from Patagonia. *Bulletin of the American Museum of Natural History*, *87*, 217–270.

Colbert, E. H., & Mook, C. C. (1951). The ancestral crocodilian *Protosuchus*. *Bulletin of the American Museum of Natural History*, *97*, 143–182.

Cope, E. D. (1869). Synopsis of the extinct Batrachia, Reptilia, and Aves of North America. *Transactions of the American Philosophical Society*, *40*, 1–252.

Crompton, A. W., & Smith, K. K. (1980). A new genus and species of crocodilian from the Kayenta Formation (Late Triassic?) of Northern Arizona. In L. L. Jacobs (Ed.), *Aspects of vertebrate history: Essays in honor of Edwin Harris Colbert* (pp. 193–217). Flagstaff: Museum of Northern Arizona Press.

Crush, P. J. (1984). A late Upper Triassic sphenosuchid crocodilian from Wales. *Palaeontology*, *71*, 131–157.

Curtis, K., & Padian, K. (1999). An Early Jurassic microvertebrate fauna from the Kayenta Formation of northeastern Arizona: Microfaunal change across the Triassic-Jurassic boundary. *PaleoBios*, *19*, 19–37.

Donohoo-Hurley, L. L., Geissman, J. W., & Lucas, S. G. (2010). Magnetostratigraphy of the uppermost Triassic and lowermost Jurassic Moenave Formation, western United States: Correlation with strata in the United Kingdom, Morocco, Turkey, Italy, and eastern United States. *Geological Society of America Bulletin*, *122*, 2005–2019.

Dufeau, D. L., & Witmer, L. M. (2015). Ontogeny of the middle-ear air-sinus system in *Alligator mississippiensis* (Archosauria: Crocodylia). *PLoS One*, *10*, e0137060.

Erb, A., & Turner, A. H. (2021). Braincase anatomy of the Paleocene crocodyliform *Rhabdognathus* revealed through high resolution computed tomography. *PeerJ*, *9*, e11253.

Fernández, M. S., Carabajal, A. P., Gasparini, Z., & Chong Díaz, G. (2011). A metriorhynchid crocodyliform braincase from northern Chile. *Journal of Vertebrate Paleontology*, *31*, 369–377.

Fiorelli, L., & Calvo, J. O. (2008). New remains of *Notosuchus terrestris* Woodward, 1896 (Crocodyliformes: Mesoeucrocodylia) from Late Cretaceous of Neuquén, Patagonia, Argentina. *Arquivos do Museu Nacional, Rio de Janeiro*, *66*, 83–124.

Foffa, D., Johnson, M. M., Young, M. T., Steel, L., & Brusatte, S. L. (2019). Revision of the Late Jurassic deep-water teleosauroid crocodylomorph *Teleosaurus megarhinus* Hulke, 1871 and evidence of pelagic adaptations in Teleosauroidea. *PeerJ*, *7*, e6646.

Fonseca, P. H. M., Martinelli, A. G., Marinho, T. D. S., Ribeiro, L. C. B., Schultz, C. L., & Soares, M. B. (2020). Morphology of the endocranial cavities of *Campinasuchus dinizi* (Crocodyliformes: Baurusuchidae) from the Upper Cretaceous of Brazil. *Geobios*, *58*, 1–16.

Gauthier, J. (1986). Saurischian monophyly and the origin of birds. *Memoirs of the California Academy of Sciences*, *8*, 1–55.

Gauthier, J., & Padian, K. (1985). Phylogenetic, functional, and aerodynamic analyses of the origin of birds and their flight. In M. K. Hecht, J. H. Ostrom, G. Viohl, & P. Wellnhofer (Eds.), *The beginning of birds: Proceedings of the international Archaeopteryx conference Eichstätt 1984* (pp. 185–197). Freunde des Jura Museums: Eichstätt.

Goloboff, P. A., & Catalano, S. A. (2016). TNT version 1.5, including a full implementation of phylogenetic morphometrics. *Cladistics*, *32*, 221–238.

Goloboff, P. A., Farris, J. S., Källersjö, M., Oxelman, B., Ramírez, M. J., & Szumik, C. A. (2003). Improvements to resampling measures of group support. *Cladistics*, *19*, 324–332.

Goloboff, P. A., Pittman, M., Pol, D., & Xu, X. (2019). Morphological data sets fit a common mechanism much more poorly than DNA sequences and call into question the Mkv model. *Systematic Biology*, *68*, 494–504.

Gow, C. E. (2000). The skull of *Protosuchus haughtoni*, an Early Jurassic crocodyliform from southern Africa. *Journal of Vertebrate Paleontology*, *20*, 49–56.

Grigg, G. C., & Kirshner, D. (2015). *Biology and evolution of crocodylians*. Melbourne, Australia: CSIRO and Cornell University Press.

Hay, O. P. (1930). *Second bibliography and catalogue of the fossil Vertebrata of North America*. Washington, DC: Carnegie Institution.

Herrera, Y., Fernández, M. S., & Gasparini, Z. (2013). The snout of *Cricosaurus araucanensis*: A case study in novel anatomy of the nasal region of metriorhynchids. *Lethaia*, *46*, 331–340.

Herrera, Y., Leardi, J. M., & Fernández, M. S. (2018). Braincase and endocranial anatomy of two thalattosuchian crocodylomorphs and their relevance in understanding their adaptations to the marine environment. *PeerJ*, *6*, e5686.

Herriott, T. M., Crowley, J. L., Schmitz, M. D., Wartes, M. A., & Gillis, R. J. (2019). Exploring the law of detrital zircon: LA-ICP-MS and CA-TIMS geochronology of Jurassic forearc strata, Cook Inlet, Alaska, USA. *Geology*, *47*, 1044–1048.

Hesselbo, S. P., Ogg, J. G., Ruhl, M., Hinnov, L. A., & Huang, C. J. (2020). The Jurassic Period. In F. M. Gradstein, J. G. Ogg, M. D. Schmitz, & G. M. Ogg (Eds.), *Geologic Time Scale 2020* (pp. 955–1021). Amsterdam: Elsevier.

Hoffman, E., & Rowe, T. B. (2018). Jurassic stem-mammal perinates and the origin of mammalian reproduction and growth. *Nature*, *561*, 104–108.

Holliday, C. M., Porter, W. R., Vliet, K. A., & Whitmer, L. M. (2020). The frontoparietal fossa and dorsotemporal fenestra of archosaurs and their significance for interpretations of vascular and muscular anatomy in dinosaurs. *The Anatomical Record*, *303*, 1060–1074.

Holloway, W. L., Claeson, K. M., & O'Keefe, F. R. (2013). A virtual phytosaur endocast and its implications for sensory system evolution in archosaurs. *Journal of Vertebrate Paleontology*, *33*, 848–857.

Irmis, R. B., Nesbitt, S. J., & Sues, H. D. (2013). Early Crocodylomorpha. *Geological Society, London, Special Publications*, *379*, 275–302.

Jenkins, F. A., Jr., Crompton, A. W., & Downs, W. R. (1983). Mesozoic mammals from Arizona: New evidence on mammalian evolution. *Science*, *222*, 1233–1235.

Johnson, M. M., Young, M. T., & Brusatte, S. L. (2020). The phylogenetics of Teleosauroidea (Crocodylomorpha, Thalattosuchia) and implications for their ecology and evolution. *PeerJ*, *8*, e9808.

Jouve, S. (2009). The skull of *Teleosaurus cadomensis* (Crocodylomorpha; Thalattosuchia), and phylogenetic analysis of Thalattosuchia. *Journal of Vertebrate Paleontology*, *29*, 88–102.

Kley, N. J., Sertich, J. J. W., Turner, A. H., Krause, D. W., O'Connor, P. M., & Georgi, J. A. (2010). Craniofacial morphology of *Simosuchus clarki* (Crocodyliformes: Notosuchia) from the Late Cretaceous of Madagascar. *Journal of Vertebrate Paleontology*, *30*, 13–98.

Lautenschlager, S., & Butler, R. J. (2016). Neural and endocranial anatomy of Triassic phytosaurian reptiles and convergence with fossil and modern crocodylians. *PeerJ*, *4*, e2251.

Leardi, J. M., Pol, D., & Clark, J. M. (2017). Detailed anatomy of the braincase of *Macelognathus vagans* Marsh, 1884 (Archosauria,

Crocodylomorpha) using high resolution tomography and new insights on basal crocodylomorph phylogeny. *PeerJ*, *5*, e2801.

Leardi, J. M., Pol, D., & Clark, J. M. (2020). Braincase anatomy of *Almadasuchus figarii* (Archosauria, Crocodylomorpha) and a review of the cranial pneumaticity in the origins of Crocodylomorpha. *Journal of Anatomy*, *237*, 48–73.

Lessner, E. J., & Stocker, M. R. (2017). Archosauriform endocranial morphology and osteological evidence for semiaquatic sensory adaptations in phytosaurs. *Journal of Anatomy*, *231*, 655–664.

Marsh, A. D. (2015). Preliminary U–Pb detrital zircon dates from the Kayenta Formation of Arizona. *PaleoBios*, *31*, 10.

Marsh, A. D. (2018). *Contextualizing the evolution of theropod dinosaurs in western North America using U–Pb geochronology of the Chinle Formation and Kayenta Formation on the Colorado Plateau* (Ph.D. dissertation), The University of Texas at Austin, Austin, Texas. 654 pp.

Marsh, A. D., Rowe, T., Simonetti, A., Stockli, D., & Stockli, L. (2014). The age of the Kayenta Formation of northeastern Arizona: Overcoming the challenges of dating fossil bone. *Journal of Vertebrate Paleontology (Online Supplement)*, *34*, 178.

Marsh, A. D., & Rowe, T. B. (2018). Anatomy and systematics of the sauropodomorph *Sarahsaurus aurifontanalis* from the Early Jurassic Kayenta Formation. *PLoS One*, *13*, e0204007.

Marsh, A. D., & Rowe, T. B. (2020). A comprehensive anatomical and phylogenetic evaluation of *Dilophosaurus wetherilli* (Dinosauria, Theropoda) with descriptions of new specimens from the Kayenta Formation of northern Arizona. *Journal of Paleontology*, *94*, 1–103.

Martínez, R. N., Alcober, O. A., & Pol, D. (2019). A new protosuchid crocodyliform (Pseudosuchia, Crocodylomorpha) from the Norian Los Colorados Formation, northwestern Argentina. *Journal of Vertebrate Paleontology*, *38*, e1491047.

Melstrom, K. M., & Irmis, R. B. (2019). Repeated evolution of herbivorous crocodyliforms during the age of dinosaurs. *Current Biology*, *29*, 2389–2395.

Molina-Garza, R. S., Geissman, J. W., & Lucas, S. G. (2003). Paleomagnetism and magnetostratigraphy of the lower Glen Canyon and upper Chinle groups, Jurassic-Triassic of northern Arizona and northeast Utah. *Journal of Geophysical Research B*, *108*, 1–23.

Moreau, M.-G., Bucher, H., Bodergat, A.-M., & Guex, J. (2002). Pliensbachian magnetostratigraphy: New data from Paris Basin (France). *Earth and Planetary Science Letters*, *203*, 755–767.

Nash, D. (1968). A crocodile from the Upper Triassic of Lesotho. *Journal of Zoology*, *156*, 163–179.

Nesbitt, S. J. (2011). The early evolution of archosaurs: Relationships and the origin of major clades. *Bulletin of the American Museum of Natural History*, *352*, 1–292.

Nesbitt, S. J., Stocker, M. R., Parker, W. G., Wood, T. A., Sidor, C. A., & Angielczyk, K. D. (2017). The braincase and endocast of *Parringtonia gracilis*, a Middle Triassic suchian (Archosaur: Pseudosuchia). *Journal of Vertebrate Paleontology*, *37*, 122–141.

Ősi, A., Young, M. T., Galácz, A., & Rabi, M. (2018). A new large-bodied thalattosuchian crocodyliform from the Lower Jurassic (Toarcian) of Hungary, with further evidence of the mosaic acquisition of marine adaptations in Metriorhynchoidea. *PeerJ*, *6*, e4668.

Osmólska, H., Hua, S., & Buffetaut, E. (1997). *Gobiosuchus kielanae* (Protosuchia) from the Late Cretaceous of Mongolia: Anatomy and relationships. *Acta Palaeontologica Polonica*, *42*, 257–289.

Owen, R. (1850). XXVII. On the communications between the cavity of the tympanum and the palate in the Crocodilia (gavials, alligators and crocodiles). *Philosophical Transactions of the Royal Society of London*, *140*, 521–527.

Padian, K. (1984). Pterosaur remains from the Kayenta Formation (?Early Jurassic) of Arizona. *Palaeontology*, *27*, 407–413.

Pierce, S. E., & Benton, M. J. (2006). *Pelagosaurus typus* Bronn, 1841 (Mesoeucrocodylia: Thalattosuchia) from the Upper Lias (Toarcian, Lower Jurassic) of Somerset England. *Journal of Vertebrate Paleontology*, *26*, 621–635.

Pierce, S. E., Williams, M., & Benson, R. B. J. (2017). Virtual reconstruction of the endocranial anatomy of the Early Jurassic marine crocodylomorph *Pelagosaurus typus* (Thalattosuchia). *PeerJ*, *5*, e3225.

Pol, D., Ji, S., Clark, J. M., & Chiappe, L. M. (2004). Basal crocodyliforms from the Lower Cretaceous Tugulu Group (Xinjiang, China), and the phylogenetic position of *Edentosuchus*. *Cretaceous Research*, *25*, 603–622.

Pol, D., & Norell, M. A. (2004). A new crocodyliform from Zos Canyon, Mongolia. *American Museum Novitates*, *3445*, 1–36.

Pol, D., Rauhut, O. W. M., Lecuona, A., Leardi, J. M., Xu, X., & Clark, J. M. (2013). A new fossil from the Jurassic of Patagonia reveals the early basicranial evolution and the origins of Crocodyliformes. *Biological Reviews*, *88*, 862–872.

Porter, W. R., Sedlmayr, J. C., & Witmer, L. M. (2016). Vascular patterns in the heads of crocodilians: Blood vessels and sites of thermal exchange. *Journal of Anatomy*, *229*, 800–824.

Rasmussen, C., Mundil, R., Irmis, R. B., Giesler, D., Gehrels, G. E., Olsen, P. E., ... Parker, W. G. (2020). U–Pb zircon geochronology and depositional age models for the Upper Triassic Chinle Formation (Petrified Forest National Park, Arizona, USA): Implications for Late Triassic paleoecological and paleoenvironmental change. *Geological Society of America Bulletin*, *133*, 539–558.

Richard, S. M., Reynolds, S. J., Spencer, J. E., & Pearthree, P. A. (2000). Geologic map of Arizona. *Arizona Geological Survey Map*, *35*, 1–5.

Sachs, S., Johnson, M. M., Young, M. T., & Abel, P. (2019). The mystery of *Mystriosaurus*: Redescribing the poorly known Early Jurassic teleosauroid thalattosuchians *Mystriosaurus laurillardi* and *Steneosaurus brevior*. *Acta Palaeontologica Polonica*, *64*, 565–579.

Schwab, J. A., Young, M. T., Neenan, J. M., Walsh, S. A., Witmer, L. M., Herrera, Y., ... Brusatte, S. L. (2020). Inner ear sensory system changes as extinct crocodylomorphs transitioned from land to water. In *Proceedings of the National Academy of Sciences of the United States of America* (Vol. *117*, pp. 10422–10428).

Sereno, P. C., & Larsson, H. C. E. (2009). Cretaceous crocodyliforms from the Sahara. *ZooKeys*, *28*, 1–143.

Sereno, P. C., Larsson, H. C. E., Sidor, C. A., & Gado, B. (2001). The giant crocodyliform *Sarcosuchus* from the Cretaceous of Africa. *Science*, *294*, 1516–1519.

Serrano-Martínez, A., Knoll, F., Narváez, I., Lautenschlager, S., & Ortega, F. (2019). Inner skull cavities of the basal eusuchian *Lohuecosuchus megadontos* (Upper Cretaceous, Spain) and neurosensorial implications. *Cretaceous Research*, *93*, 66–77.

Serrano-Martínez, A., Knoll, F., Narváez, I., Lautenschlager, S., & Ortega, F. (2020). Neuroanatomical and neurosensorial analysis

of the Late Cretaceous basal eusuchian *Agaresuchus fontisensis* (Cuenca, Spain). *Papers in Palaeontology*, *7*, 641–656.

Serrano-Martínez, A., Knoll, F., Narváez, I., & Ortega, F. (2019b). Brain and pneumatic cavities of the braincase of the basal alligatoroid *Diplocynodon tormis* (Eocene, Spain). *Journal of Vertebrate Paleontology*, *39*, e1572612.

Sertich, J. J. W., & O'Connor, P. M. (2014). A new crocodyliform from the middle Cretaceous Galula Formation, southwestern Tanzania. *Journal of Vertebrate Paleontology*, *34*, 576–596.

Steiner, M. (2014). Age of Lower Jurassic Springdale Sandstone of southwestern Utah from its magnetic polarity sequence. *Volumina Jurassica*, *12*, 23–30.

Sterli, J., & Joyce, W. G. (2007). The cranial anatomy of the Early Jurassic turtle *Kayentachelys aprix*. *Acta Palaeontologica Polonica*, *52*, 675–694.

Stocker, M. R., Nesbitt, S. J., Criswell, K. E., Parker, W. G., Witmer, L. M., Rowe, T. B., … Brown, M. A. (2016). A dome-headed stem archosaur exemplifies convergence among dinosaurs and their distant relatives. *Current Biology*, *26*, 2674–2680.

Stubbs, T. L., Pierce, S. E., Rayfield, E. J., & Anderson, S. L. (2013). Morphological and biomechanical disparity of crocodile-line archosaurs following the end-Triassic. *Proceedings of the Royal Society B*, *280*, 20131940.

Suarez, C. A., Knobbe, T. K., Crowley, J. L., Kirkland, J. I., & Milner A. R. C. (2017). A chronostratigraphic assessment of the Moenave Formation, USA using C-isotope chemostratigraphy and detrital zircon geochronology: Implications for the terrestrial end Triassic extinction. *Earth and Planetary Science Letters*, *475*, 83–93.

Sues, H.-D. (1986). The skull and dentition of two tritylodontid synapsids from the Lower Jurassic of western North America. *Bulletin of the Museum of Comparative Zoology*, *151*, 217–268.

Sues, H.-D., Clark, J. M., & Jenkins, F. A. (1994). A review of the Early Jurassic tetrapods from the Glen Canyon Group of the American Southwest. In *In the shadow of the dinosaurs: Early Mesozoic tetrapods* (pp. 284–294). Cambridge, MA: Cambridge University Press.

Sues, H.-D., Olsen, P. E., Carter, J. G., & Scott, D. M. (2003). A new crocodylomorph archosaur from the Upper Triassic of North Carolina. *Journal of Vertebrate Paleontology*, *23*, 329–343.

Toljagic, O., & Butler, R. J. (2013). Triassic–Jurassic mass extinction as trigger for the Mesozoic radiation of crocodylomorphs. *Biology Letters*, *9*, 20130095.

Tykoski, R. S. (2005). Vertebrate paleontology in the Arizona Jurassic. *Mesa Southwest Museum Bulletin*, *11*, 72–93.

Tykoski, R. S., Rowe, T. B., Ketcham, R. A., & Colbert, M. W. (2002). *Calsoyasuchus valliceps*, a new crocodyliform from the Early Jurassic Kayenta Formation of Arizona. *Journal of Vertebrate Paleontology*, *22*, 593–611.

von Quadt, A., Gallhofer, D., Guillong, M., Peytcheva, I., Waelle, M., & Sakata, S. (2014). U–Pb dating of CA/non-CA treated zircons obtained by LA-ICP-MS and CA-TIMS techniques: Impact for their geological interpretation. *Journal of Analytical Atomic Spectrometry*, *29*, 1618–1629.

Walker, A. A. D. (1990). A revision of *Sphenosuchus acutus* Haughton, a crocodylomorph reptile from the Elliot Formation (Late Triassic or Early Jurassic) of South Africa. *Philosophical Transactions of the Royal Society of London Series B: Biological Sciences*, *330*, 1–120.

Watanabe, A., Gignac, P. M., Balanoff, A. M., Green, T. L., Kley, N. J., & Norell, M. A. (2019). Are endocasts good proxies for brain size and shape in archosaurs throughout ontogeny? *Journal of Anatomy*, *234*, 291–305.

Whetstone, K. N., & Whybrow, P. J. (1983). A "cursorial" crocodilian from the Triassic of Lesotho (Basutoland), southern Africa. In *Occasional papers of the museum of natural history* (Vol. 106, pp. 1–37). The University of Kansas, Lawrence, Kansas.

Wilberg, E. W. (2015). What's in an outgroup? The impact of outgroup choice on the phylogenetic position of Thalattosuchia (Crocodylomorpha) and the origin of Crocodyliformes. *Systematic Biology*, *64*, 621–627.

Wilberg, E. W., Turner, A. H., & Brochu, C. A. (2019). Evolutionary structure and timing of major habitat shifts in Crocodylomorpha. *Scientific Reports*, *9*, 514.

Wu, X., & Chatterjee, S. (1993). *Dibothrosuchus elaphros*, a crocodylomorph from the Lower Jurassic of China and the phylogeny of the Sphenosuchina. *Journal of Vertebrate Paleontology*, *13*, 58–89.

Wu, X., Sues, H.-D., & Dong, Z.-M. (1997). *Sichuanosuchus shuhanensis*, a new? Early Cretaceous protosuchian (Archosauria: Crocodyliformes) from Sichuan (China), and the monophyly of Protosuchia. *Journal of Vertebrate Paleontology*, *17*, 89–103.

Wu, X.-C., Russell, A. P., & Cumbaa, S. L. (2001). *Terminonaris* (Archosauria: Crocodyliformes): New material from Saskatchewan, Canada, and comments on its phylogenetic relationships. *Journal of Vertebrate Paleontology*, *21*, 492–514.

Yang, Z., Moreau, M.-G., Bucher, H., Dommergues, J.-L., & Trouiller, A. (1996). Hettangian and Sinemurian magnetostratigraphy from Paris Basin. *Journal of Geophysical Research B*, *101*, 8025–8042.

Zittel, K. A. (1887–1890). *Handbuch der Palaeontologie. 1. Abteilung: Palaeozoologie, 3*. München & Leipzig.

SUPPORTING INFORMATION

Additional supporting information may be found in the online version of the article at the publisher's website.

How to cite this article: Melstrom, K. M., Turner, A. H., & Irmis, R. B. (2021). Reevaluation of the cranial osteology and phylogenetic position of the early crocodyliform *Eopneumatosuchus colberti*, with an emphasis on its endocranial anatomy. *The Anatomical Record*, 1–26. https://doi.org/10.1002/ar.24777